# *Simulation of tracked wheels on soft soil substrates*

## 1. Summary

Multiple analysis strategies were applied to the problem of simulating a tracked wheel on soft soils, with the ultimate goal of generating results that could be compiled into Context Models (C2M2L) for the DARPA Advanced Vehicle Make project. These strategies included:

- Finite Element Analysis
- FEA using eroding solid elements
- SPH (Smoothed Particle Hydrodynamics) technology
- SPH technology utilizing adaptive solid elements

None of the strategies worked perfectly. All of these approaches seem to work reasonably well with firm substrates but until very recently all have encountered significant issues with contact instabilities during the analyses of soft, highly deformable soils. These issues led us to concentrate our efforts on the FEA and SPH strategies while prematurely terminating efforts to implement strategies with eroding solid elements and adaptive solid-SPH elements. Very recently (6-Dec-2012), we began evaluating a fix from LSTC support personnel (new parameter values) that shows great promise in solid element problems but has not corrected the issue in SPH analyses. There, the instabilities affect many (but not all) of the analyses, usually late in the computations. The results from analyses that have completed are encouraging.

Out of the above approaches, SPH still shows the most promise for being able to address the case of soft soils in spite of the contact instabilities. The results from simulations of a simple tracked wheel on several different soil types demonstrated the qualitative differences one would expect between soft and hard materials and demonstrated the qualitative differences one would expect when the analysis was performed on sloped domains and with higher acceleration rates. A substantial increase in SPH mesh density may also be required (with corresponding increase in CPU resources) for the quantitative results necessary to distinguish between different track designs.

A variant of the SPH strategy, the Adaptive SPH technology of LS-DYNA is also, in principle, an ideal way to approach the problem but only preliminary efforts were made to incorporate it before being discouraged by the contact instabilities and turning our attention to other methods. There will still be a need for close interaction/training with LSTC to make effective use of it and tailor the relevant method parameters correctly.

FEA with erosion, with the contact issue under control, appears to be a tractable method but the results will be dependent upon the proper selection of the element failure criteria. The result of using low failure thresholds, while accurate in principle, may result in excessive element removal from the model effectively removing the substrate from the model altogether, compromising the approach significantly.

## 1.1 Technical Challenges

A significant and persistent issue with contact instabilities during the analyses of soft, highly deformable substrates has affected our ability to complete the evaluation of any of the above solution strategies. The instability manifested itself as the sudden appearance of a very strong, anomalous force in the system, dramatically distorting elements and usually terminating the model at that time. The instability would typically not occur until well into an analysis making the debugging and determination of what was really happening time consuming and tedious. More importantly, as the issue first arose in problems involving erosion (eroding solid and adaptive solid-SPH analyses) it was believed that the problem rose from those methods and not, as later determined by LSTC, from generic contact instabilities. This resulted in a redirection of efforts away from these strategies until very recently.

During the course of the project we have had numerous interactions with LSTC support on the appropriate contact settings to use for both solid-solid contact and SPH-solid contact definitions. Usually the issues were minor and correctable. The suggested fixes have all had the effect of slowing model execution due to reduced time step and more robust contact search algorithms but none of the fixes were able to overcome the instability issue. We have attempted to validate the latest fix from LSTC support personnel (new parameter values) and while the new values give an improvement in our ability to analyze solid element problems it has not corrected the issue in SPH analyses. In fact, they seem to have made things worse in those analyses. Still, we are optimistic that this can be resolved and allow more extensive SPH models to be evaluated in future work.

The choices of appropriate material models and data sets were unspecified at the start of the project. While there is no one model or data set that can represent the wide range of substrates that the tracked wheels could conceivably encounter we believe that we have accumulated an appropriate selection of soil types to test the model rigorously.

The use of eroding solid elements appears to be a viable but risky strategy for analyzing soft soils. One of the keys to a successful erosion model is the proper selection of erosion criteria and parameter values. These parameters and criteria for erosion are not necessarily available for most material models and the selection of parameter values is often *ad hoc*, reducing confidence in the quantitative accuracy of the models (Schwer, 2012). . Also extreme caution needs to be used to ensure that the technique is not excessively removing substrate from the model.

CPU requirements for the relatively coarse mesh models analyzed here have been moderate (generally 1-2 days for SPH models, ½ day for FEA models). However, to increase the SPH mesh density to the level needed to quantitatively resolve different track pad geometries we need to be able to handle models with roughly 100-1000X more nodes. Executing models of this size for extensive work such as Design Of Experiments investigations will require a significant amount of CPU resources.

  

## 1.2 General Methodology

Multiple analysis strategies were applied to the problem of simulating a tracked wheel on soft soils. These strategies included:

- Finite Element Analysis
- FEA using eroding solid elements
- SPH (Smoothed Particle Hydrodynamics) technology
- SPH technology utilizing adaptive solid elements

In considering the interaction of a tracked wheel on soils our main concern was having a capability for dealing with extreme deformation or destruction of the soil with large amounts of the substrate likely thrown clear of the immediate vicinity in such a way that any remeshing approach would likely find itself overwhelmed. For a Lagrangian approach such as Finite Element Analysis this would quickly lead to either termination of the model due to severe mesh distortion or the ignoring of substantial changes in the geometrical domain due to substrate dispersal.

There are analysis methodologies for dealing with situations that encounter the problem of severe mesh distortion that fall into a class referred to as "mesh-free" techniques. One of these techniques, Smoothed Particle Hydrodynamics, (SPH) has been implemented in some mainstream FEA codes (Hallquist, 2006) and has been successfully used in a number of problems involving soils (see, for example, (Kulak & Schwer, 2012) or (Lescoe, 2010)) and should be applicable to our situation. Many of the relevant journal or conference articles using SPH with solid materials are utilizing it in relatively high-speed events where mass dominates over other physical considerations which also would seem to be appropriate for our situation. LS-DYNA, a general-purpose explicit structural analysis finite element code from LSTC was used for all calculations as it has the comprehensive capabilities to address all anticipated analysis techniques (FEA, SPH (Guo, 2010)) and a diverse group of constitutive relations for different soil types. A further advantage of using LS-DYNA is that, being an explicit time-stepping code, the memory requirements are significantly lower than those of an implicit code.

While not all constitutive relations in LS-DYNA are available for SPH materials many of the relevant soil models are. Performing an SPH analysis requires a modest amount of additional information and setup detail, including the specification of an Equation of State to address the pressure-volume relationship in compression.

About half way through the project we became aware of a feature available in more recent versions of LS-DYNA (V971, Rev 5.1.1 or later) that at first glance looks like an even more convenient implementation of SPH technology. In this feature, the substrate areas where interaction with the tracked wheel is anticipated can be meshed with solid elements which are also flagged. When these flagged elements "fail" they are converted to SPH nodes which are then, depending upon the choice of the analyst, free to "couple" or not with the remaining solid elements. Until that time, they behave as regular solid continuum elements. In other words, we should be able to perform a regular Lagrangian analysis when the substrates are strong and firm (presumably more accurate than using SPH elements) but the material will convert to SPH elements under high stress/deformation and allow the analysis to adapt to that situation and carry on. This was also one of the approaches used.

  

While remeshing of the Lagrangian domain was not an approach implemented in this work we did investigate the use of LS-DYNA's element erosion capability to see if that could be a useful technique. In that approach, elements are deemed to have "failed" when a specified parameter reaches a user-specified threshold. At that time the element is removed from the calculation, creating either voids or new free surfaces. This approach is described in more detail in the following section.

Lastly, primarily as a control, simulations were also performed using a straightforward FE analysis to see just how severe the element distortion problem would be for the different substrate types.

For each of these approaches the goal and initial strategy was the same. A simple validation model was constructed with a simple, tracked wheel on top of a substrate under a gravitational load. After a short time period (0.5-2 sec) for stabilization the wheel would be rotationally accelerated to a modest velocity (~10 MPH center-of-mass) with the torque necessary and actual wheel center-of-mass translational velocity calculated in the program as output quantities. In particular, we wanted to see how far the wheel would compress the soil during the stabilization period. Would the wheel dig into the substrate and displace any material from the model and how that varied for the different soil data sets available were other questions to be answered by the model. As we gained confidence in the models, complexity would be added to the analysis. First, additional soil models and data sets would be analyzed and later, actual track designs would be used in the simulation as well as more demanding types of analyses (sloped domains, braking tests). Then it would be possible to start extracting overall performance metrics from the models and to start to build a database of performance characteristics for the C2M2L Context models.

### 1.2.1 Details of the Calculations

A wide variety of constitutive models in LS-DYNA have been used in SPH simulations of soils. One of the simpler models, Material Type 5 (Soil and Foam) has been used for the vast majority of the calculations here. In addition to its simplicity this material type has multiple data sets available for appropriate substrates. The data sets available from all constitutive models are summarized in Section 1.7 as an Annex but the majority of the work done here was done using Material Type 5, data sets 4-6 and 8 which are soils or sands ranging from soft to firm. The most recent sets used are from a study (Chitty, 2011) of sand and soil types at the Kennedy Space Center that were explicitly characterized with LS-DYNA material Type 5 in mind. In the results, specific mention is made as to which material model and data set were used.

A further advantage of the Type 5 material model is that there is an associated model in LS-DYNA (Type 14, Soil and Foam Failure) which uses the same data as Type 5 but allows LS-DYNA to make use of the Pressure Cutoff value (point at which the material can no longer hold tension) as a failure criterion for erosion. This was used as part of the work in implementing element erosion as was the use of the *MAT_ADD_EROSION command, where LS-DYNA allows one to define their own erosion criteria. This latter approach was used with a trigger value of -3.4475 KPa for MNPRES (minimum pressure) which corresponds to the PC (pressure cutoff) parameter in Material Type 5 for most data sets.

An equation of state is required in SPH analyses to address the pressure-volume relationship in compression. For the Type 5 or 14 materials this is addressed by the P vs. ln (vol. strain) data. For other constitutive models a specific EOS must be chosen from the number of models available in LS-DYNA. Most of the EOS models in LS-DYNA are designed to be compatible with shock waves. Due to the relatively low-speed nature of track/substrate interactions (very low Mach number) the simplest form of EOS is all that is required. For those constitutive models that required an EOS we used the simplest representation (Linear Polynomial) with only non-zero coefficient C2=K (bulk modulus).

Friction coefficients of 0.3 were used for both static and dynamic values, representing a typical value between soil and metal (Tekeste, Raper, Tollner, & Way, 2005).

The units used in all of the calculations were all in the mm-mN-kg-sec system. A simple tracked wheel design was created (Figure 1) for use in this study with properties (steel, rubber) taken from the I-DEAS library:

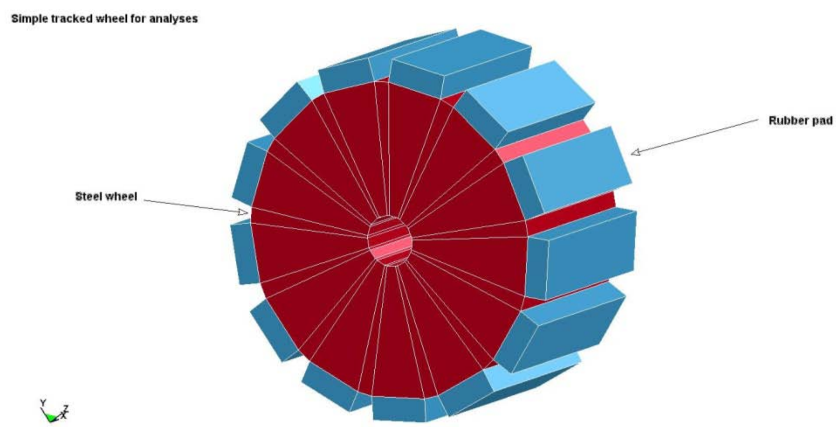


Figure 1 – Tracked steel wheel with 13 equally spaced rectangular rubber pads

The wheel has an overall diameter of roughly 726 mm with the pads measuring 338x105x75 mm. A 101.6 mm section at the center of the wheel was removed. In LS-DYNA, this volume is replaced by a rigid cylindrical body (also of steel) which is used to drive the wheel via a nodal constraint (rotational velocity and load curve). Nodes at the boundary between the rigid body and the wheel deliver the total X-moment needed to accelerate and drive the wheel.

While not an actual tracked wheel design this initial geometry would still be capable of addressing the relevant physics of the interaction between soft soils and hard geometries that can bite into the substrate. A very crude mesh was used to represent the wheel and the pads as these entities were expected to act as semi-rigid bodies with respect to the substrates.

A number of different mesh densities and geometrical designs for the substrate domain were used in the course of the project. As an example of one of the later constructions, Figure 2 shows the wheel in proximity to the substrate which has the upper 500 mm of its 2x2x1 m domain comprised of SPH elements. Note that the size of the SPH elements is only for visualization purposes and that the intended direction of travel for the wheel is in the negative-Y direction, with gravity acting in the negative-Z direction. In all models, the wheel has been placed as close as possible to top surface of substrate (<1 mm).

  

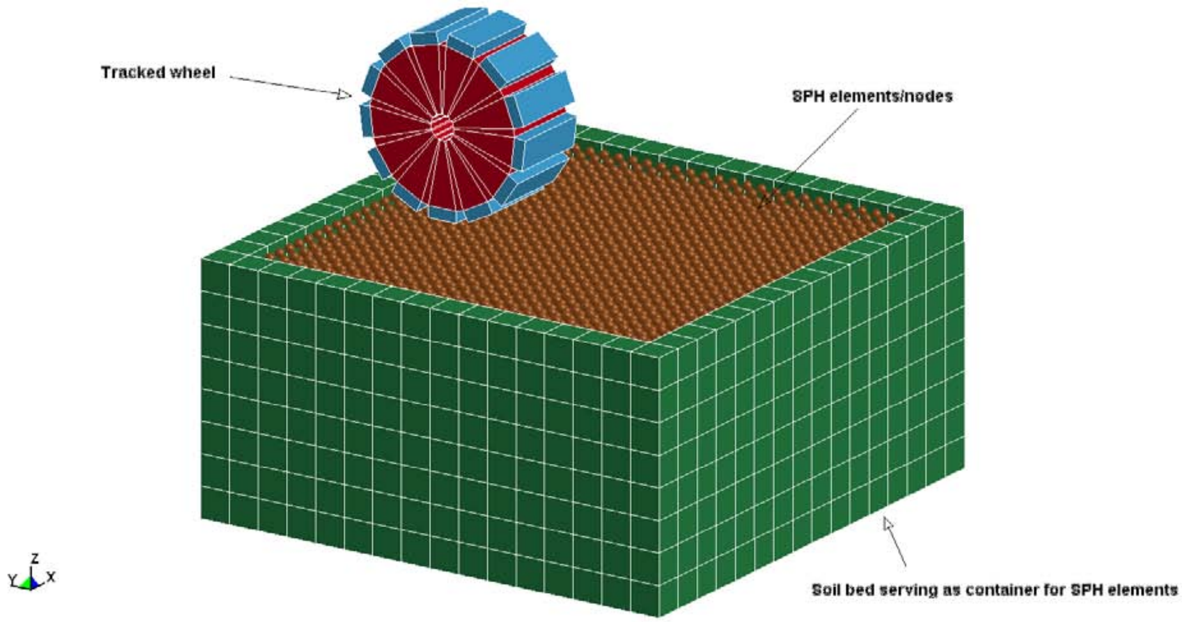


Figure 2 – Tracked wheel with on SPH substrate

One feature of the mesh is that it is relatively coarse in the SPH region (despite having over 6K nodes in the above model) as shown below in Figure 3:

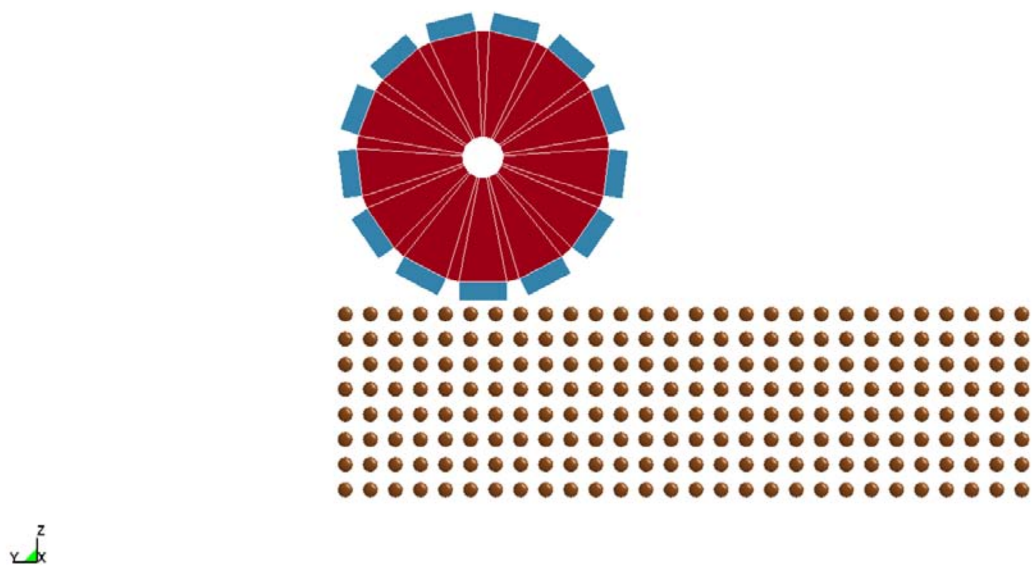


Figure 3 – Tracked wheel with on SPH substrate

With an SPH nodal spacing somewhat greater than the spacing between the pads we did not expect that this mesh could quantitatively distinguish between track pad designs without significant refinement. However, for our initial purposes we believe that the mesh density in all areas is adequate while still allowing for reasonable model computation times (~24-48 hrs for an SPH analysis; less for solid element FEA) although a proper mesh convergence study on these analyses has not yet been performed.

Boundary conditions are straightforward. The nodes on the bottom of the substrate (lowest Z-values) were clamped in all 3 principal directions. The sides were constrained to prevent any normal motion and gravity was applied from the beginning in the negative Z-direction. The wheel is constrained from moving in the X-direction but is allowed to move freely in the other two directions.

The analyses begin with a stabilization period (0.5-2 sec) to allow the system to adjust to the gravitational load and, particularly for soft soil models, to settle as needed. After this period the rotational velocity of the wheel was linearly accelerated (using the rigid body) so that the desired wheel translational velocity would be reached in the desired time. These accelerations corresponded to:

| Final angular velocity | Center of mass velocity | Time for acceleration |
| --- | --- | --- |
| 12.3 rad/sec | 4470 mm/sec (10 MPH) | 1.6 sec |
| 30.785 rad/sec | 11176 mm/sec (25 MPH) | 4.0 sec |

Given the small geometrical size of the model all the analyses save one were done using the lower velocity and even there it was assumed that the wheel would rotate past the end of the domain before reaching top speed. This was considered acceptable as in these first calculations we were most interested in the qualitative differences between models in the initial phase of the acceleration and in keeping the size of the domain (and CPU execution times) manageable.

## 1.3 Technical Results

Finite element analyses were performed on several different substrates to see how a mainstream technique would fare with these soils. For the firmer materials, the results were reasonable and show qualitative differences in behavior between the materials. Figure 4 shows the permanent deformation and plastic strain left by the wheel travelling across the surface of sand substrate (Kennedy Space Center dry sand, material type 5/data set 8):

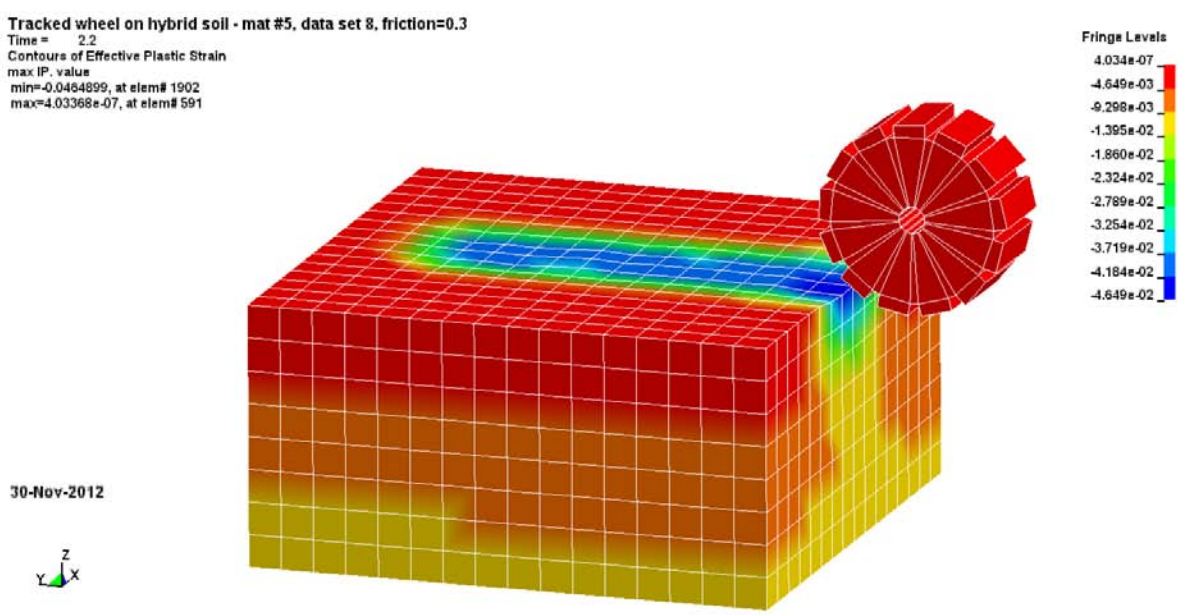

Figure 4 – Plastic strain in KSC dry sand after tracked wheel passage

There is minimal disturbance of the substrate. The next two images (Figures 5a, 5b) show the X-moment (torque) on the wheel and the translational velocity of the wheel center as functions of time:

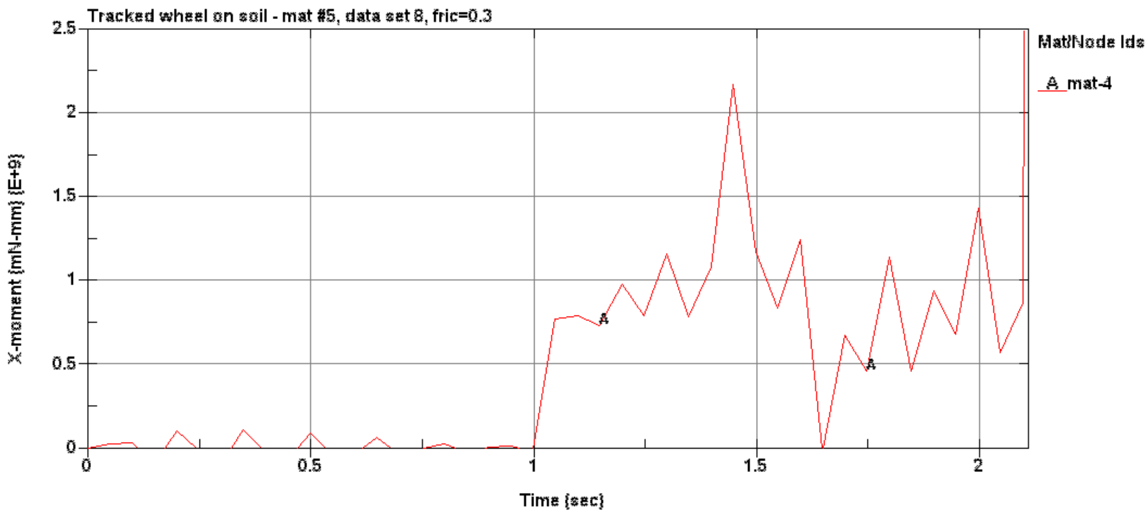


Figure 5a – X-moment on wheel hub

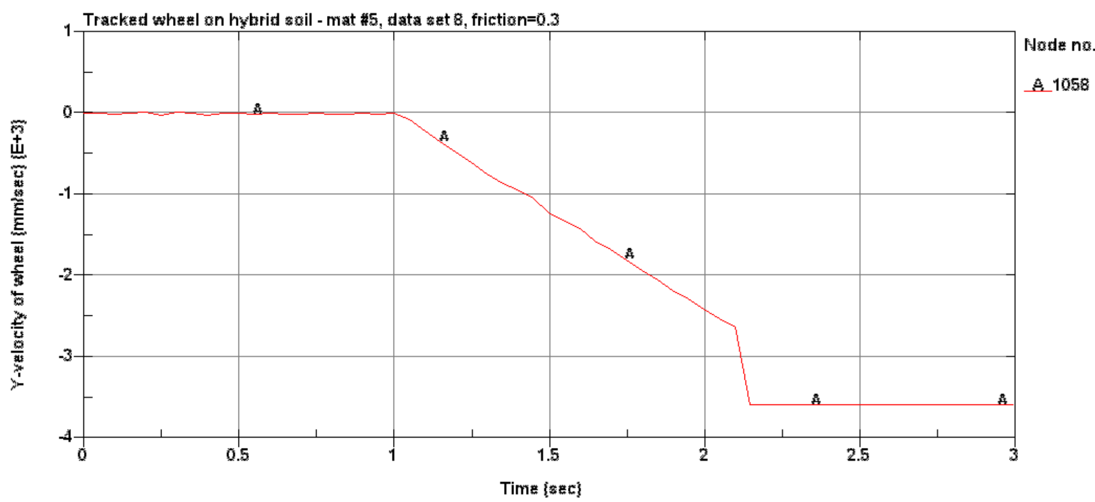


Figure 5b – Y-velocity of wheel

The results for the X-moment are quite noisy, possibly as a result of the track pads impacting the surface. The overall level of torque (roughly 1.E9 mN-mm) is about a factor of 3 greater than the torque required to accelerate the wheel in the absence of any wheel-substrate interaction (3.32E8 mN-mm) which seems reasonable. The velocity graph shows a steady acceleration towards the target of 4470 mm/sec until the wheel hits the edge of the domain. It is apparent that the wheel would not have achieved that target value by the end of the acceleration period (1-2.6 sec). This is due to the friction coefficients being set to 0.3, reducing the effective translational acceleration. The same model using a moist, dense sand (Mason sand, 15% moisture, Material Type 5 data set 9) as the substrate shows a very similar pattern for plastic strain in Figure 6:

  

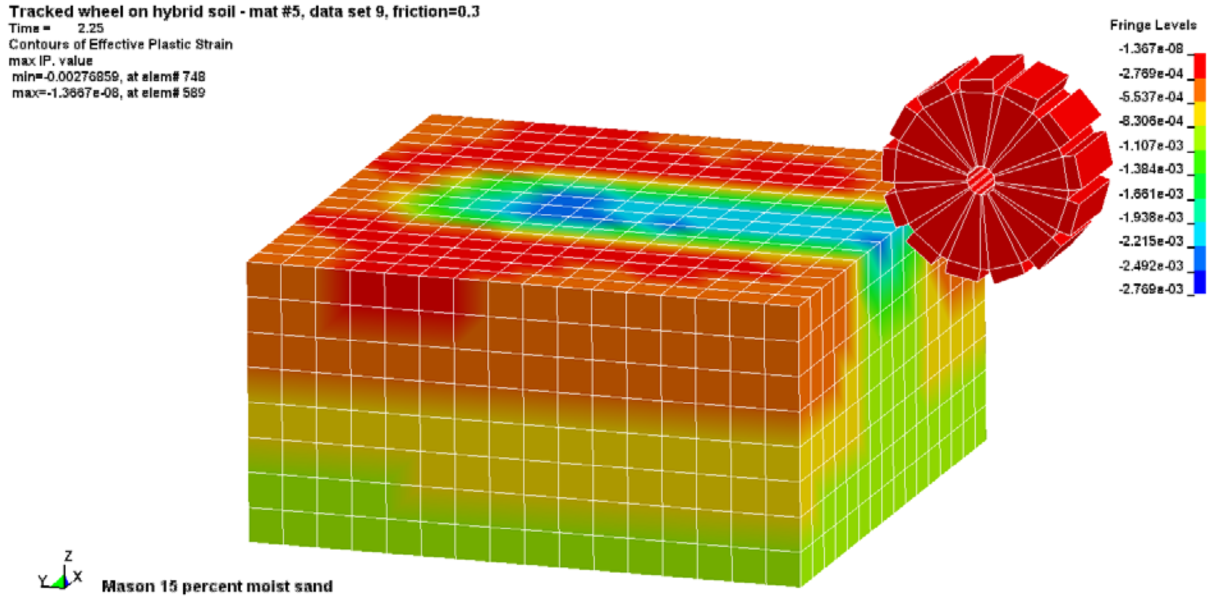


Figure 6 – Plastic strain in Mason 15% moist sand

There is a tiny amount of plastic strain in the sand; the highest amount where one of the pads impacted the surface during rotation. Plots for X-moment and Y-velocity are similar to the previous results:

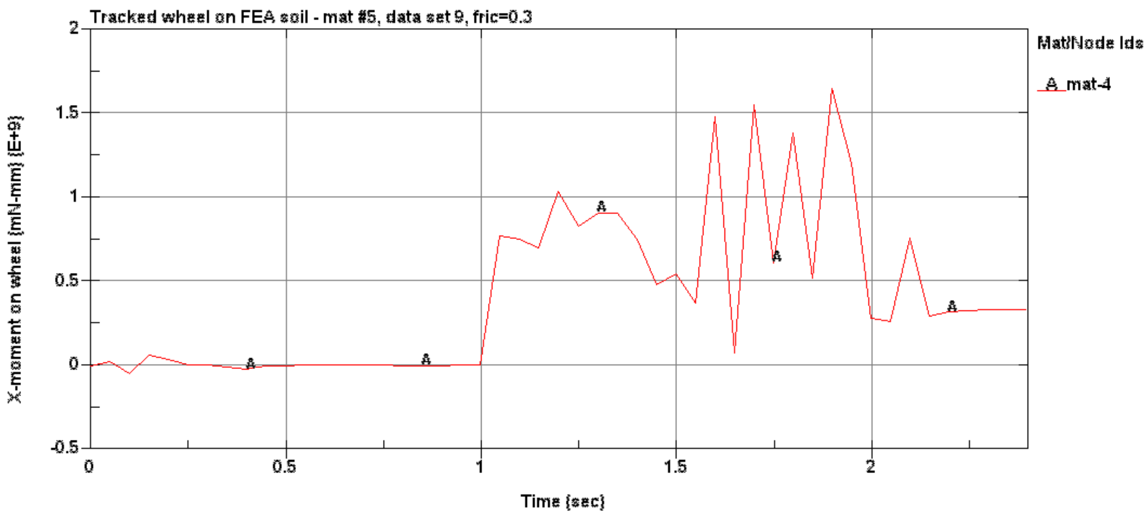


Figure 7a – X-moment on wheel hub

  

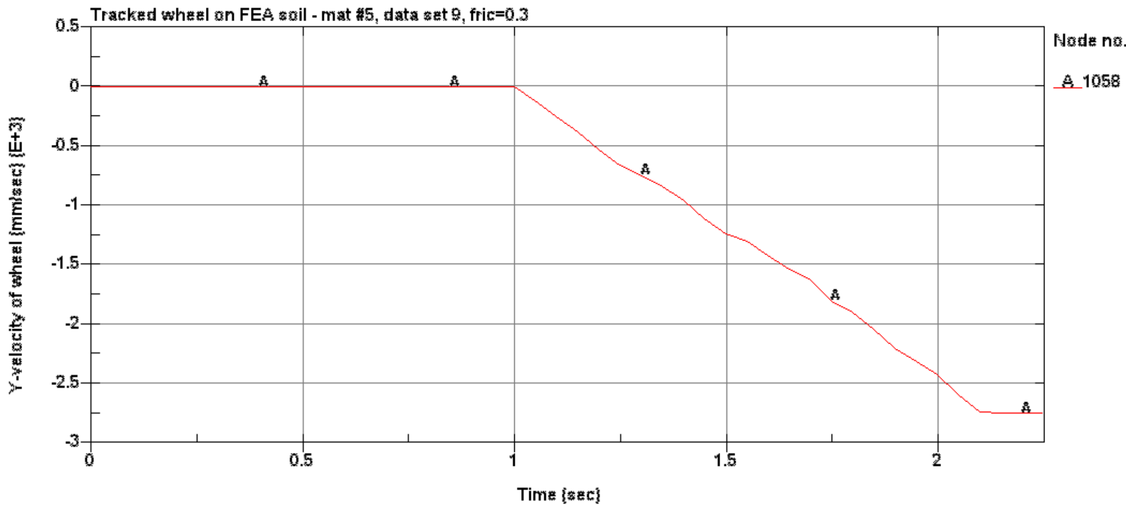


Figure 7b – Y-velocity of wheel

The quality of the results changes when soft substrates are analyzed. Figure 7c shows the deformed geometry from an analysis of a soft soil ("Fasanella soft soil"):

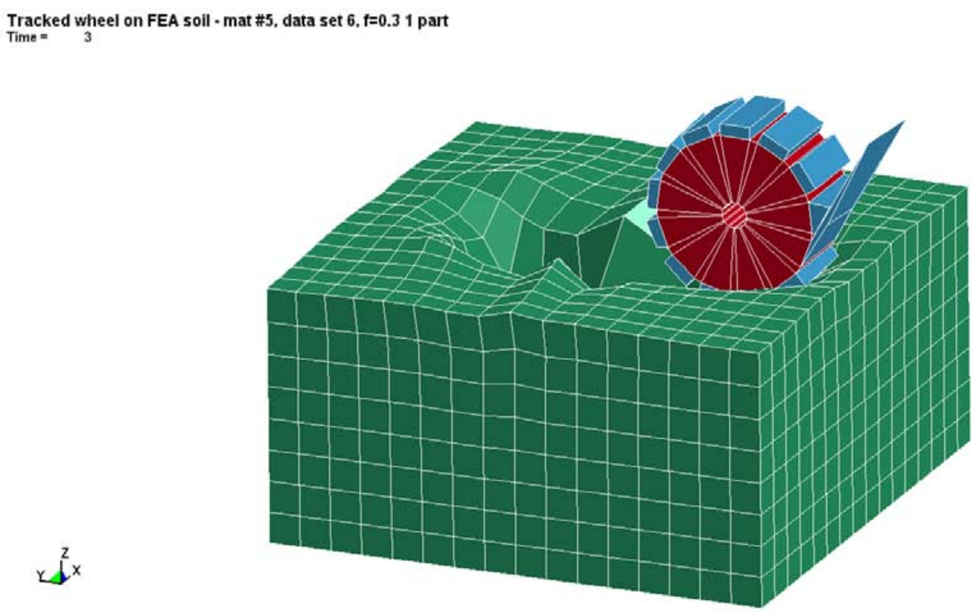


Figure 7c – Deformed geometry during analysis of Material Type 5, data set 6 (soft soil)

Here, an anomalously large force suddenly manifested itself in the system with severe deformation of some soil elements as well as one of the track pads. This was determined by LSTC support to be a contact instability. Utilizing the new Contact parameter set the final deformed geometry is much more reasonable:

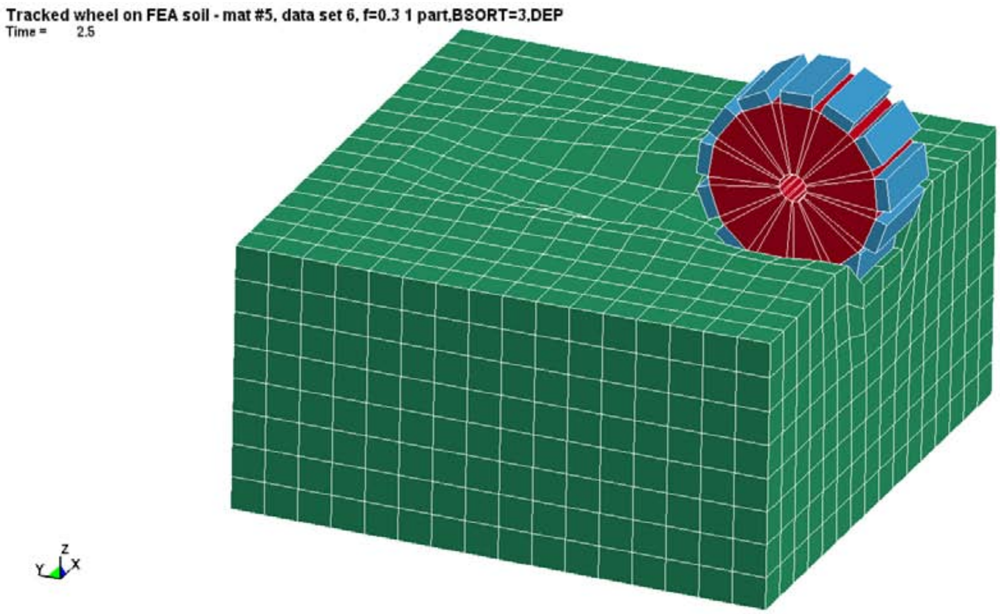


Figure 7d – Deformed geometry during analysis of Material Type 5, set 6 with new parameters

In general, the substrate deformations observed are not severe for the above mesh density, constitutive models and data sets but we anticipate some situations where there will be much more deformation than that shown above. Also, the technique and material models used above do not allow for element failure. In the meantime, using a straightforward FEA analysis we appear to have a viable method for analyzing the interactions between tracked wheels and firm substrates.

As an enhancement to the capabilities of a straightforward FEA model we made use of the eroding capability in LS-DYNA, via the *MAT_ADD_EROSION command. This command allows for the specification of multiple failure criteria for a designated material model. There are some 7 choices; at the suggestion of LSTC support personnel we eventually selected the MNPRES (minimum pressure at failure) parameter as being the closest in physical nature to the PC parameter in the Type 5 (Soil and Foam) material model.

Significant difficulties were encountered in trying to implement this approach. The most significant issue was the contact instability issue with the sudden appearance of anomalous forces in the model which caused tremendous deformation of the mesh and often caused the heavy steel wheel to be propelled backwards and upwards, as was seen during some of the non-eroding FEA analyses. Despite working with LSTC support to try and correct this behavior we were never able to eliminate it until very recently and that affected how we perceived this method in our search for a robust analysis technique. An example of the phenomena is shown in Figures 8a-d where the model is shown over a sequence of output steps. After digging a trench in the material due to erosion (using the MNPRES variable and a setting of -3.4475 KPa, the PC value from the data set) the wheel is stopped in its tracks and one of the rubber track pads is massively distorted:

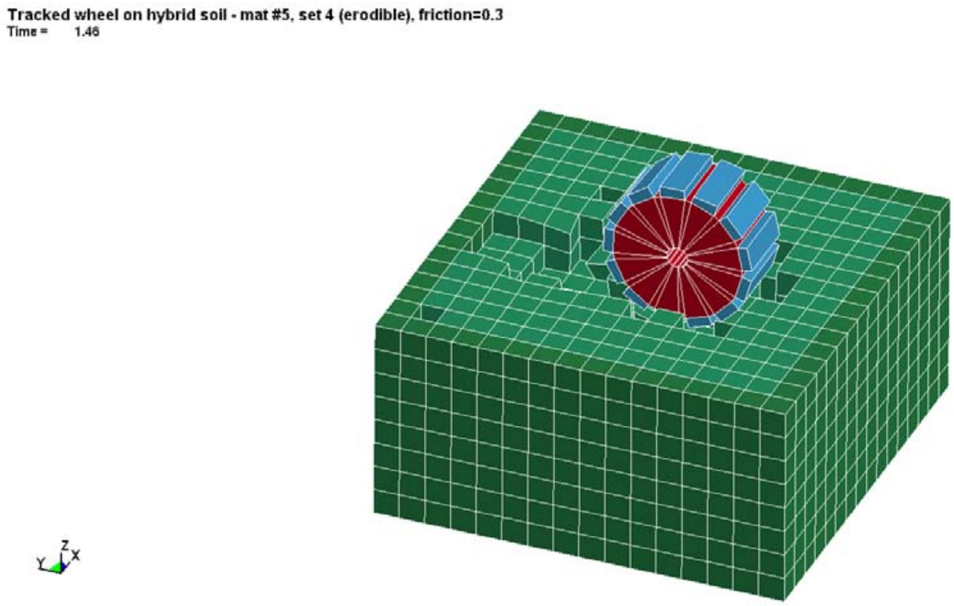


Figure 8a

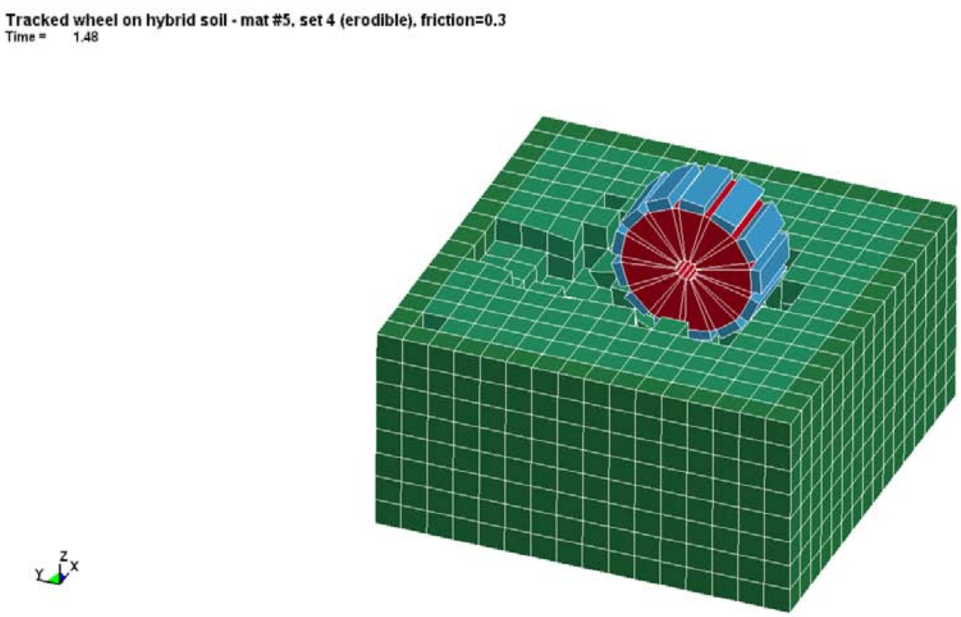


Figure 8b

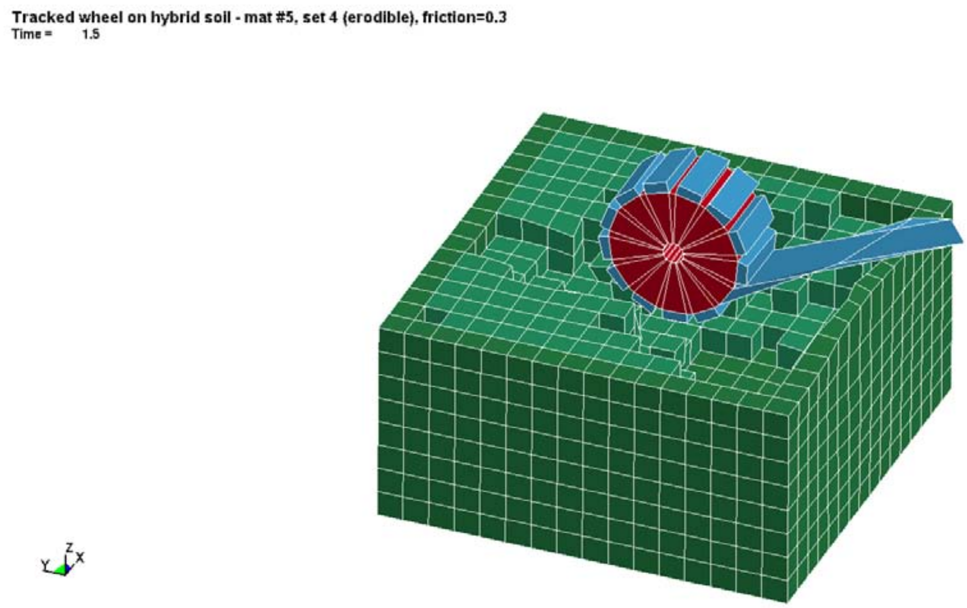


Figure 8c

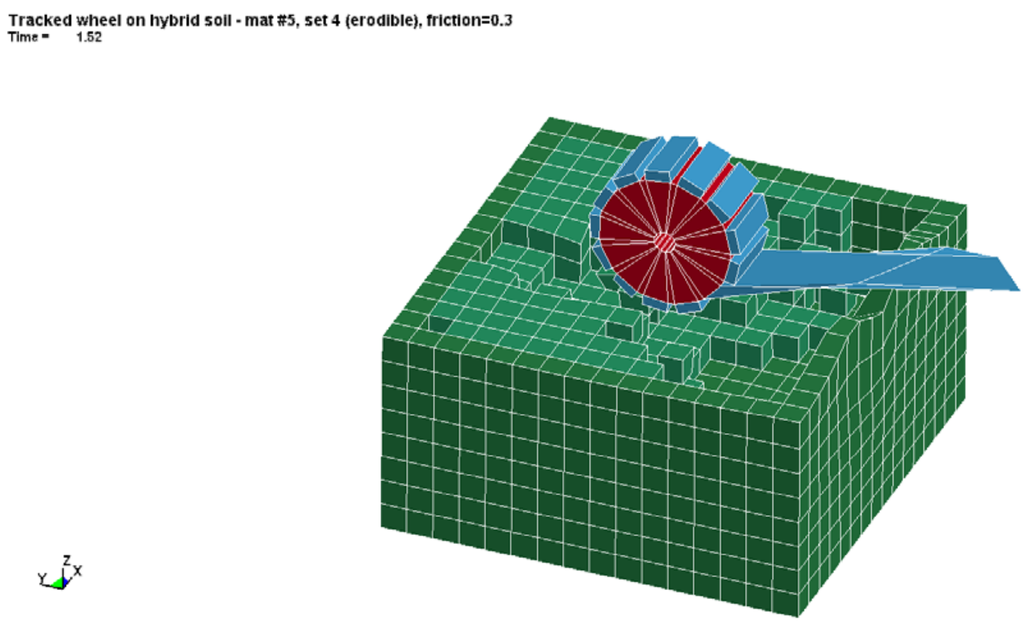


Figure 8d – Eroding contact model using Material Type 5, data set 4 (loose clay sand)

This occurred with the majority of eroding analyses where any erosion occurs and resulted in our not pursuing this technique aggressively.

After receiving the new Contact parameters mentioned previously we re-ran the above model and the results (Figure 8e) looks much more reasonable:

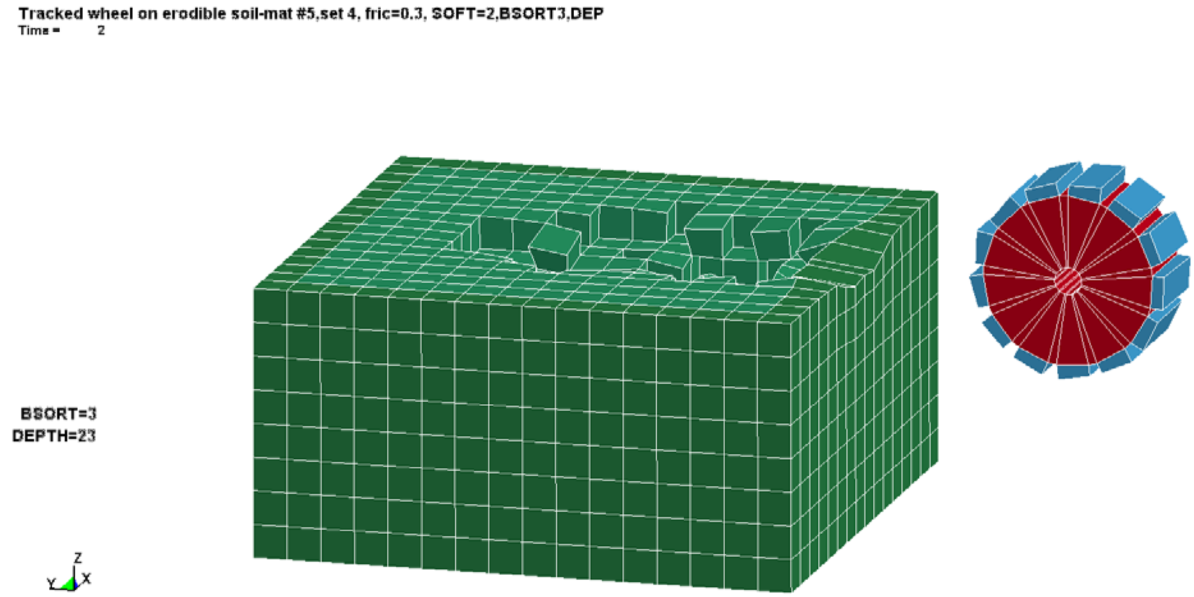


Figure 8e - Eroding contact model using Material Type 5, data set 4 (loose clay sand) and new contact parameters

The instabilities appear to have been avoided in this model and we are optimistic that this approach can now be pursued more vigorously.

While the contact instability issue affected many of the models run with soft substrates, we were occasionally lucky enough to avoid the effect and obtained interesting results. Figure 9 below shows the aftermath of running a simulation of Material Type 5, data set 8 (KSC dry sand) where the wheel has run passed through the entire domain leaving many eroded elements and substantial mesh deformation in its wake:

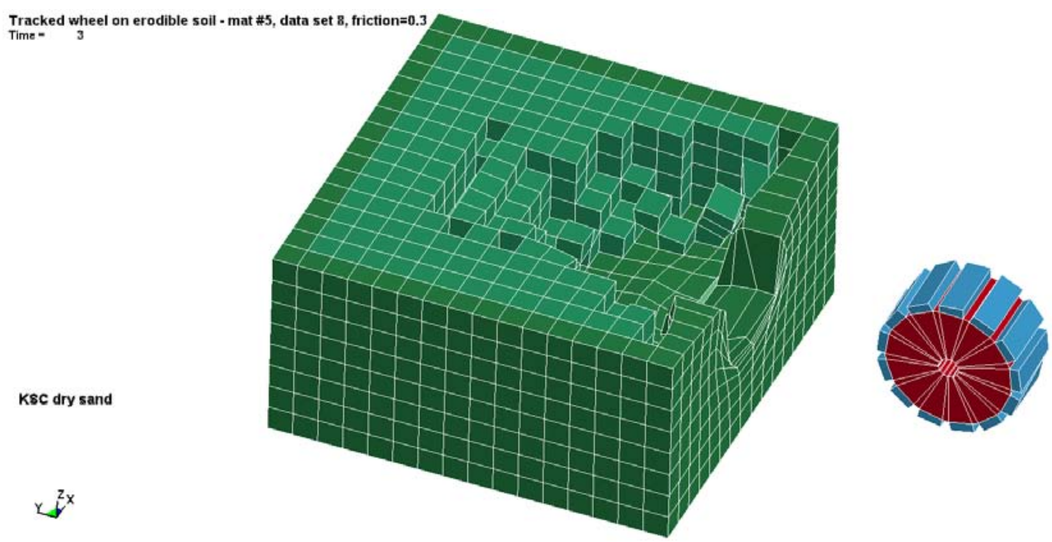


Figure 9 – Deformation after erodible contact model using KSC dry sand

This model was also re-run with the new parameter values and the result looks very much like the above:

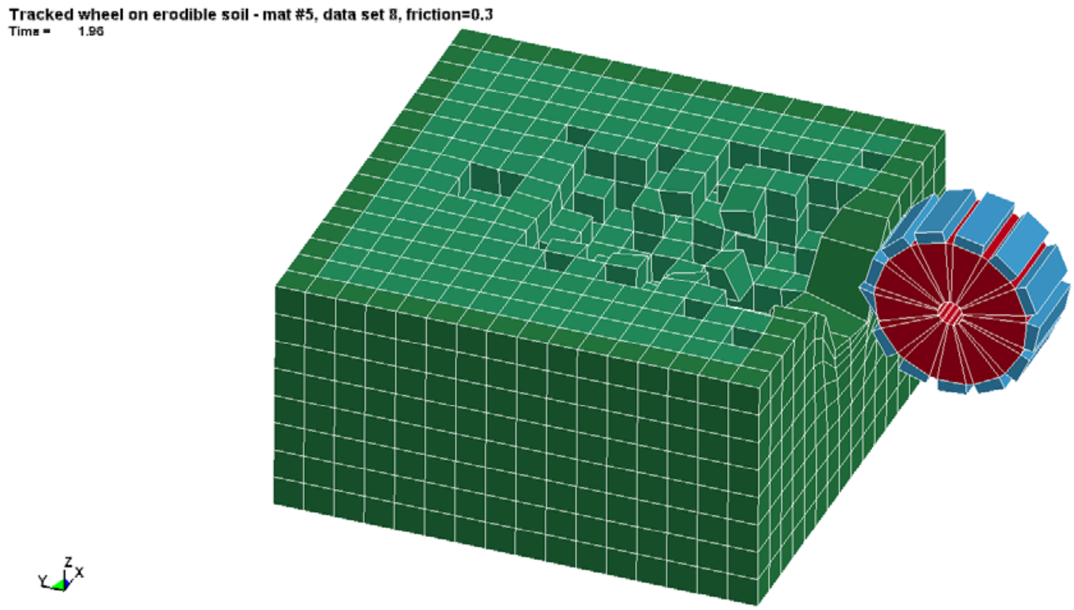


Figure 9a – Deformation after erodible contact model using KSC dry sand and new Contact parameters

Poor quality results, like those in Figures 8a-d, were obtained with other material models as well. As time was growing short on the project, this approach was put on hold. One suggestion the LSTC support personnel had made that was only just implemented was to significantly refine the erodible mesh. This suggestion made sense as each element that erodes in the above mesh has a significant effect upon the geometry, although a significantly finer mesh would have a correspondingly greater demand for CPU resources. The above model was re-run using a substantially refined mesh (4X increase in mesh density in each direction). Below, a sequence of images showing the movement of the wheel and erosion of elements highlights one of the shortcomings of the erosion technique; as the elements fail and are removed from the mesh, their locations become holes in the model and no longer resist the motion of the wheel in any way. In reality, even a totally fractured solid would still have mass that would resist the impact of the wheel. With this effect missing, the wheel simply sinks out of sight into and through the substrate as all the elements ahead of it have been determined to have failed and have been removed from the model.

  

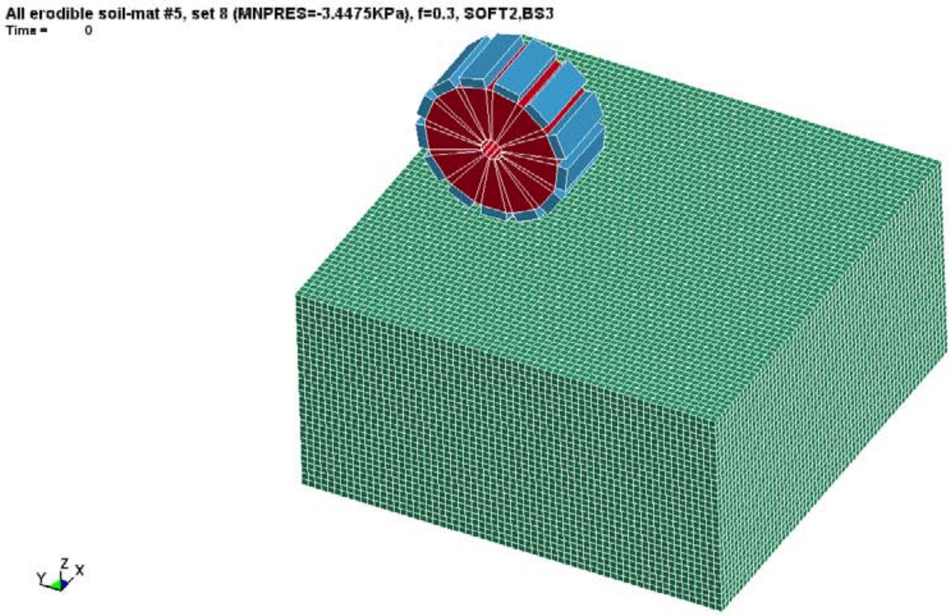


Figures 9b – Wheel on eroding soil (Material type 5, data set 8) at beginning of model

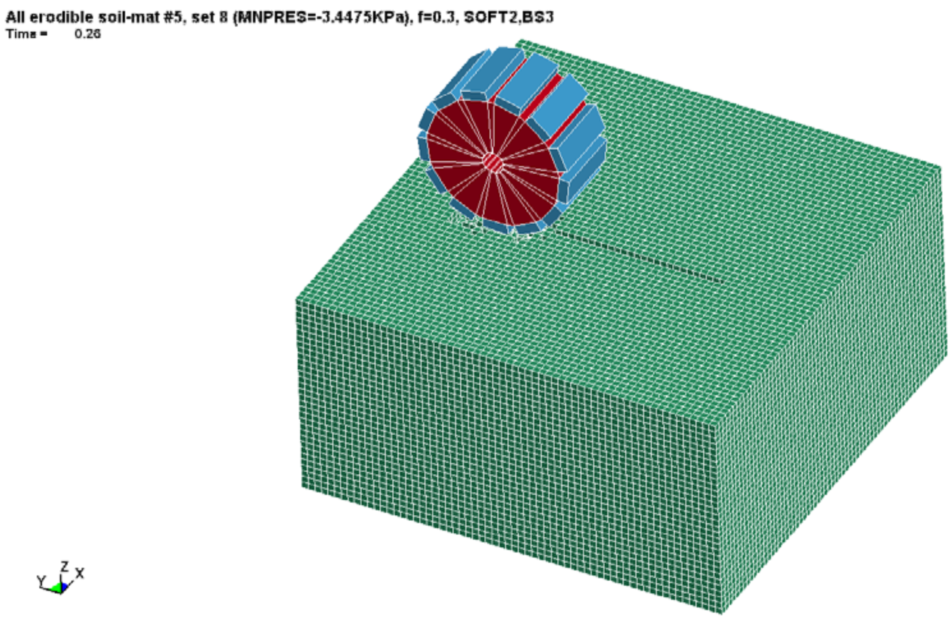


Figures 9c – Wheel on eroding soil (Material type 5, data set 8) at end of stabilization period

 

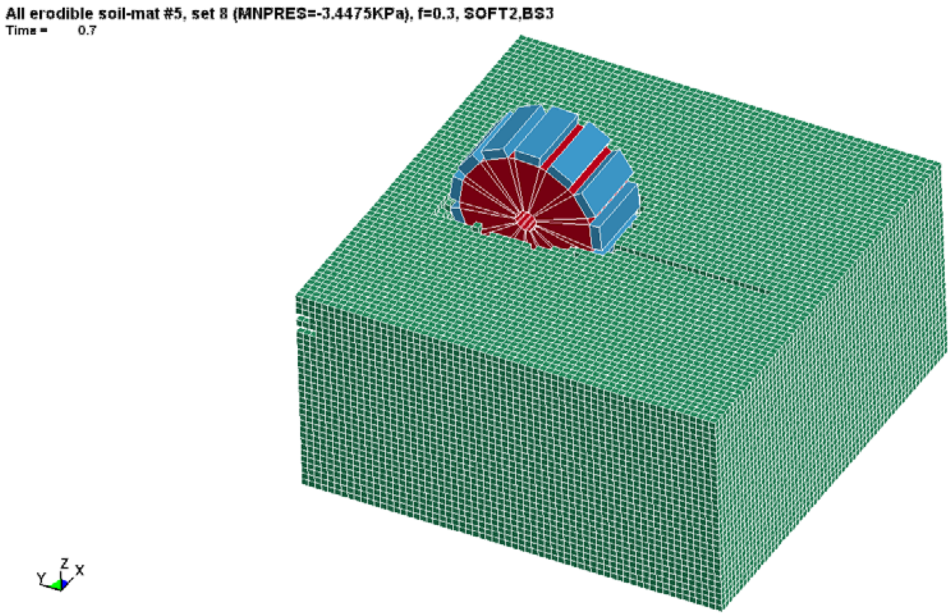


Figures 9d – Wheel on eroding soil (Material type 5, data set 8) begins rotating and digging into soil

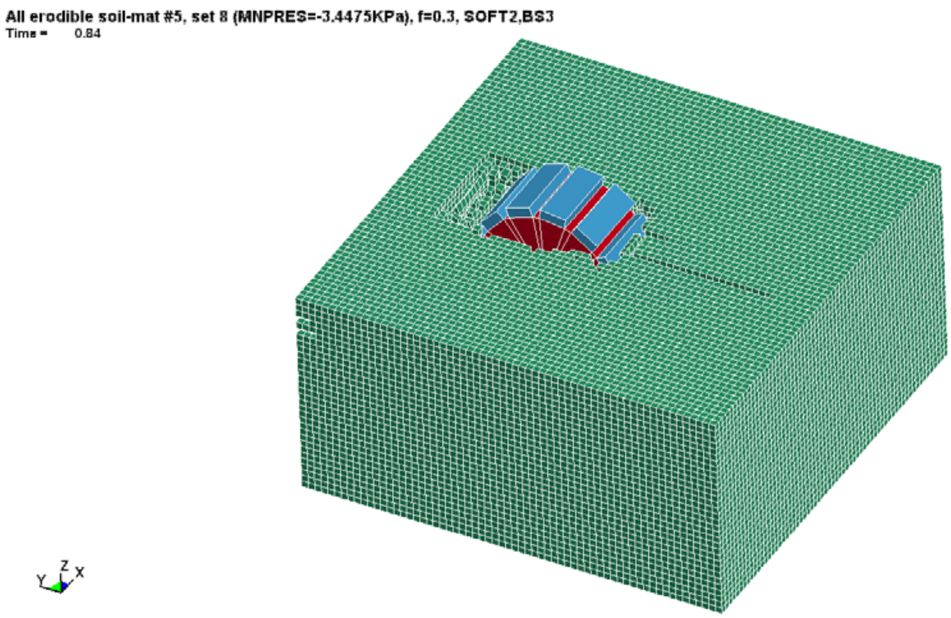


Figures 9e– Wheel on eroding soil (Material type 5, data set 8) digs further into soil

  Refer to cover page for Distribution Statement.

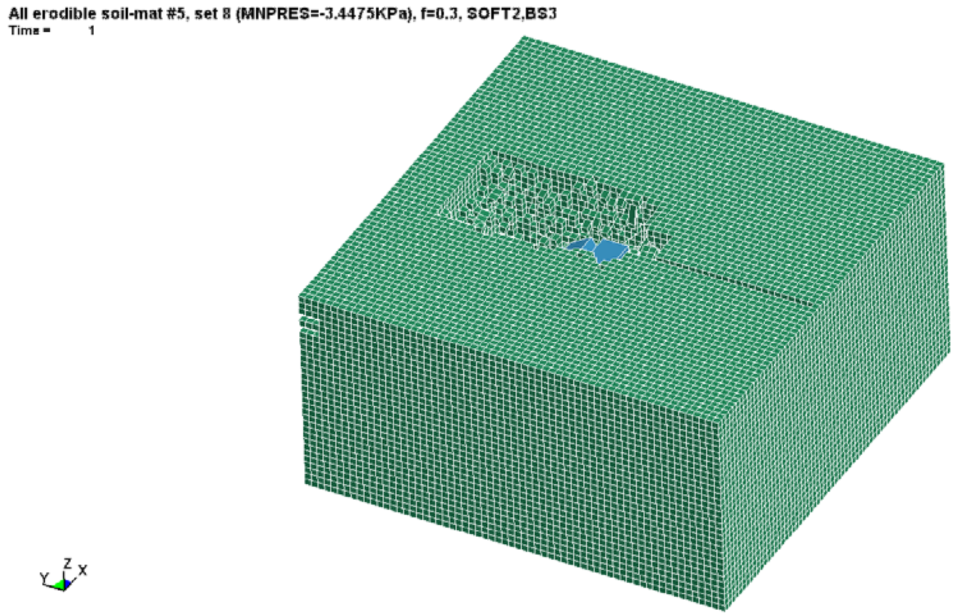


Figures 9f – Wheel on eroding soil (Material type 5, data set 8) sinks out of sight into soil

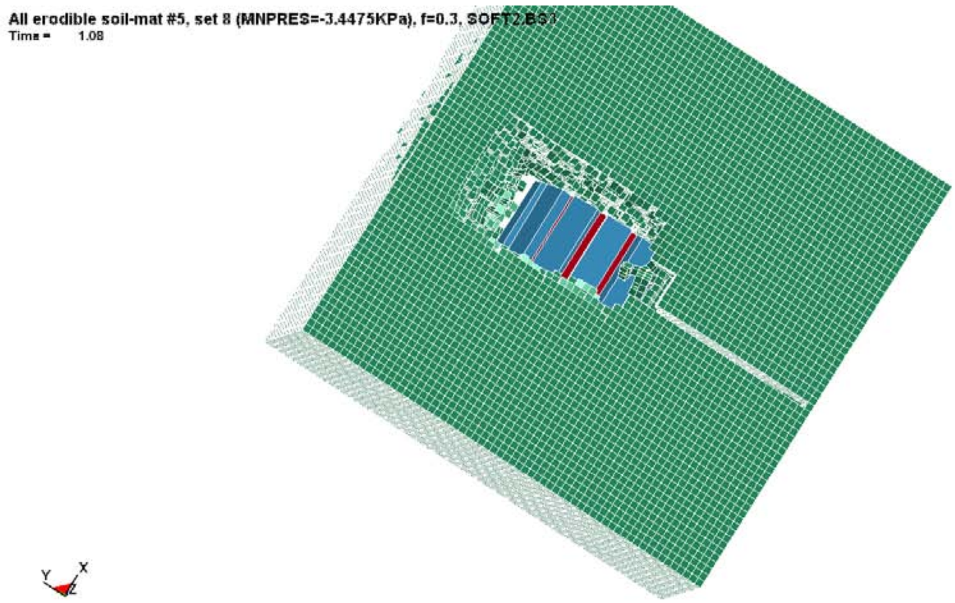


Figures 9g – Wheel on eroding soil (Material type 5, data set 8) sinks through past bottom of model

  

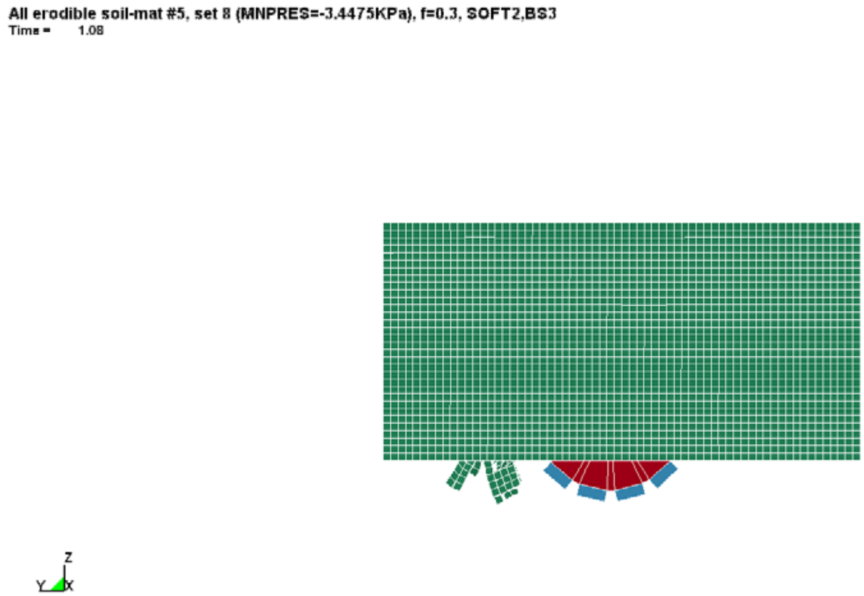


Figures 9h – Wheel on eroding soil (Material type 5, data set 8) sinks through past bottom of model

While this effect may not happen with all soil models it is definitely a shortcoming of the approach that needs to be considered for models with low failure thresholds.

Our attempts to make use of the Adaptive-solid/SPH capability in LS-DYNA also did not yield reasonable results and suffered from the same contact instabilities as the eroding contact approach. A key concept in this technique is that, as in erodible solids, the conversion of solid elements to SPH elements takes place after an element has "failed", with the failure criteria to be decided by the user. Thus the problem is set up in much the same way as the eroding contact approach, but here the elements get converted to SPH nodes rather than disappear from the analysis and so should be more physically realistic.

Unfortunately, our issues with contact instabilities left us unable to make the approach function as we think it should. In Figure 10 the deformations of a model using a Type 5 material (data set 6, Fasanella "Soft Soil") shows how the SPH and solid meshes have been grossly distorted near the end of the 2 sec stabilization period. Elements had started to erode at about 1.80 sec and by 2.0 seconds an anomalous, massive force appeared in the model:

 

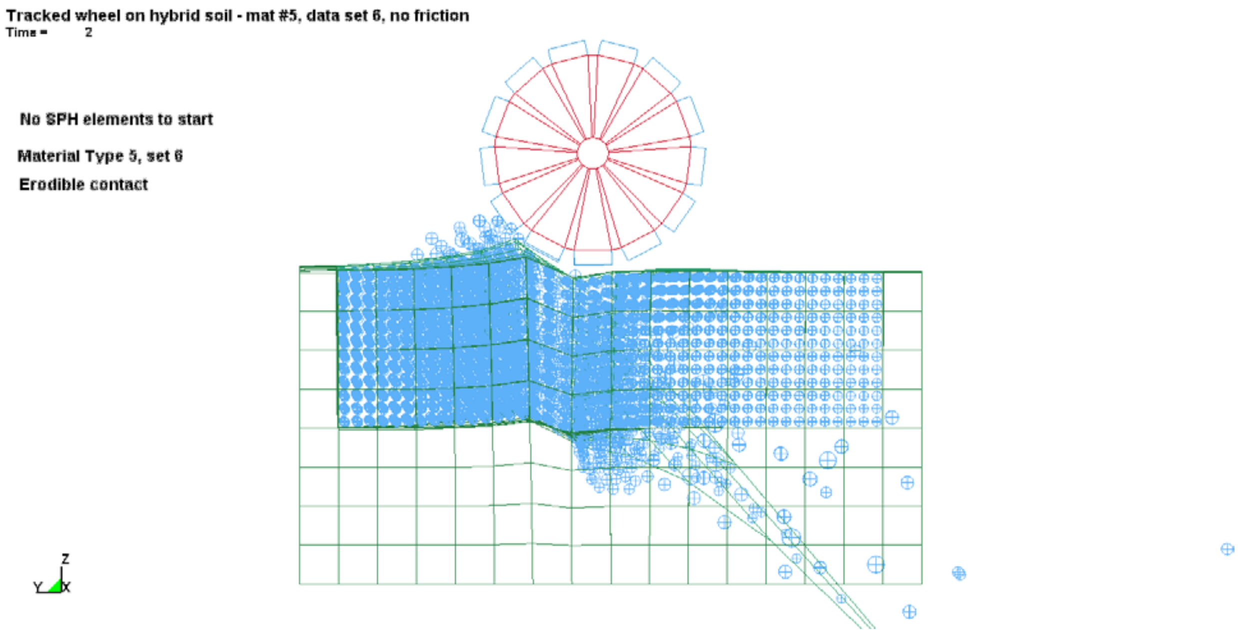


Figure 10 – Adaptive Solid to SPH model using Material Type 5, data set 6

The new LSTC Contact parameters may help correct this behavior but we have not had a chance to evaluate them in this method. Due to our inability to find a solution in a timely fashion, this approach was abandoned in favor of pursuing the SPH approach full time.

One characteristic of the SPH models is that there is almost always a little more deformation and settling due to gravity and the weight of the steel wheel than seen in a solid-element FEA mesh. Given the hydrodynamic character of the analysis this is perhaps to be expected. With an appropriate selection of the SST contact parameter, though, the issue appears to be a negligible one.

Figures 11a-c show the wheel and SPH mesh at the beginning, middle and end of an analysis using a dense, moist sand (Material Type 14, data set 9):

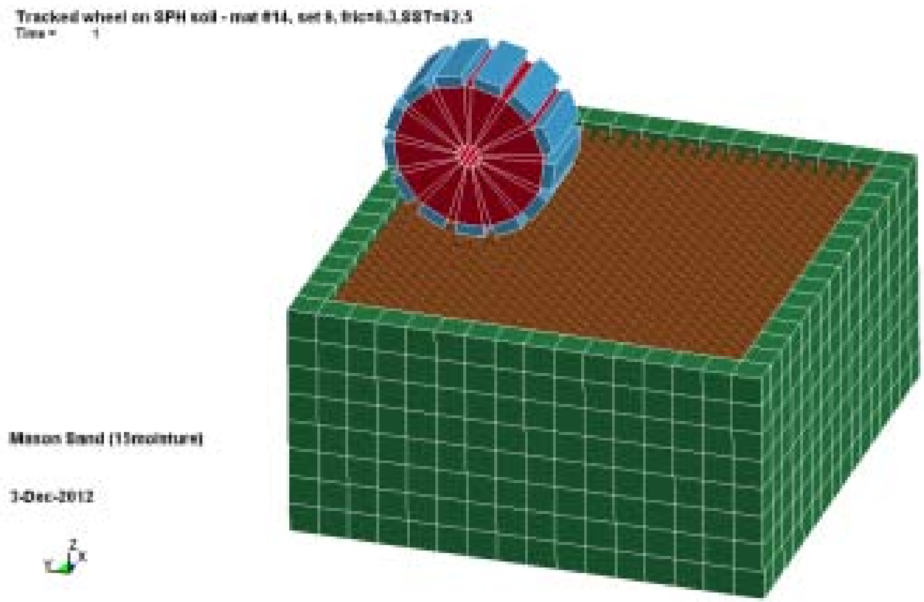


Figure 11a - Wheel at beginning of SPH analysis of Mason sand (15% moisture)

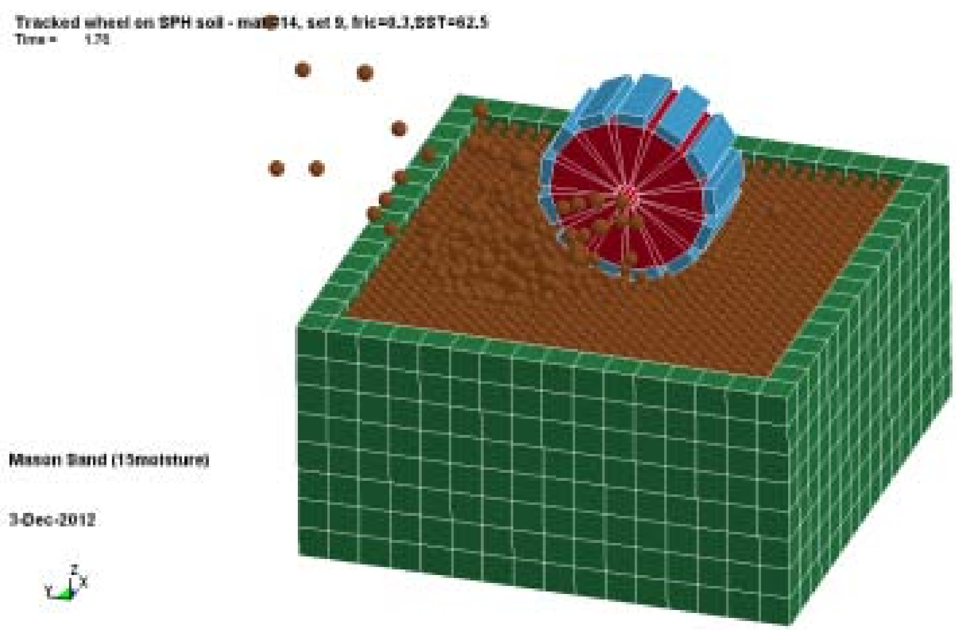


Figure 11b - Wheel at middle of SPH analysis of Mason sand (15% moisture)

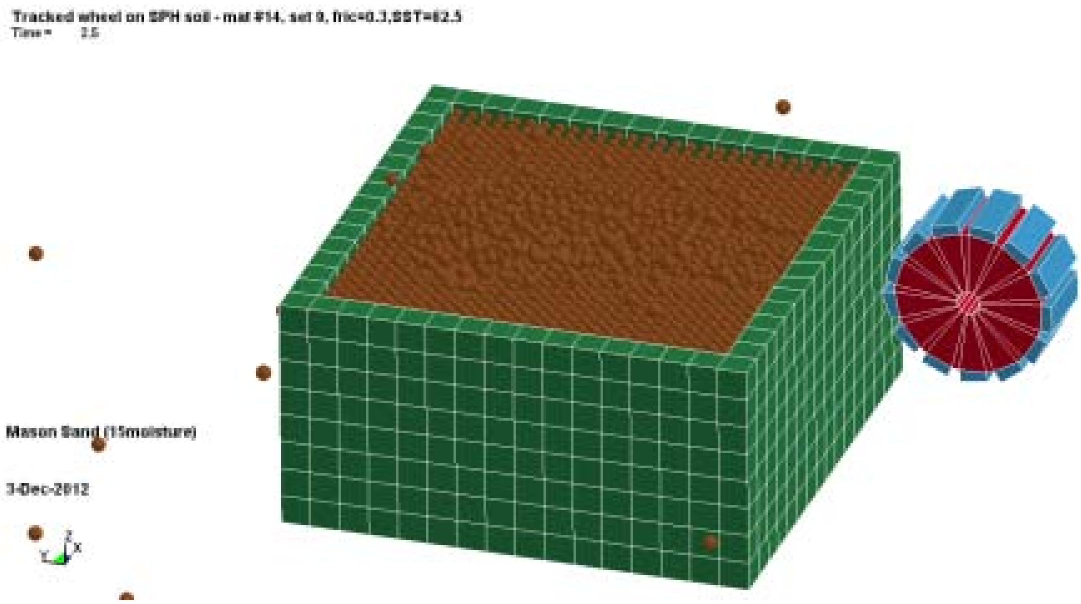


Figure 11c – Wheel at end of SPH analysis of Mason sand (15% moisture)

Here the model behaves as expected with SPH particles being thrown out of the domain as the wheel accelerates and eventually rolls off the end of the domain. Both the plastic strain and the von Mises stress in the substrate at the end of the analysis (Figures 12a-b) have reasonable values:

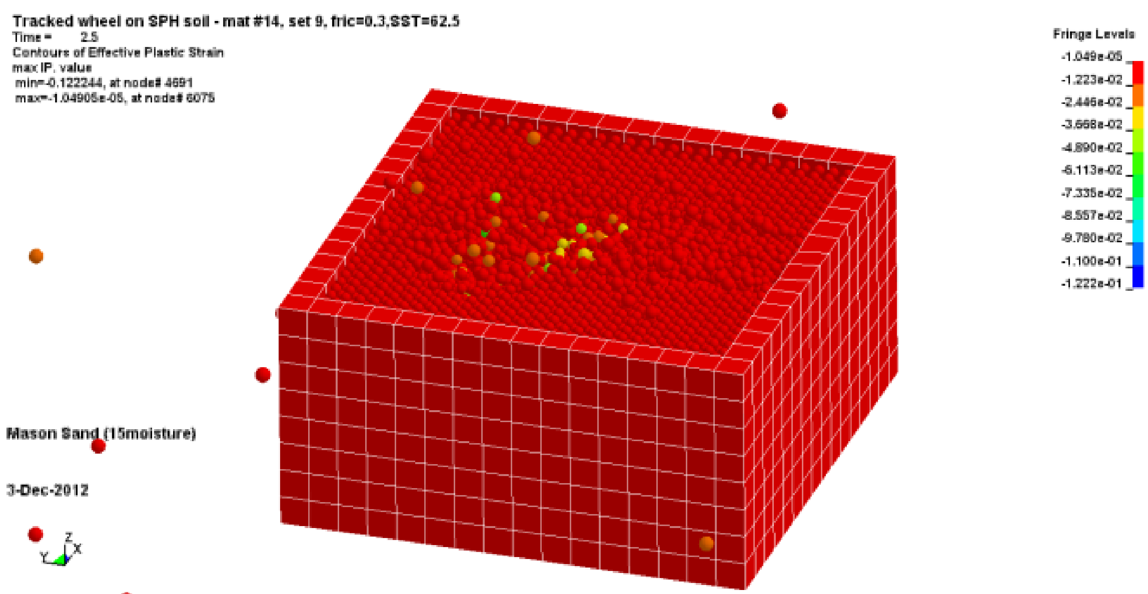


Figure 12a – Plastic strain in substrate (Mason sand, 15% moisture) after analysis

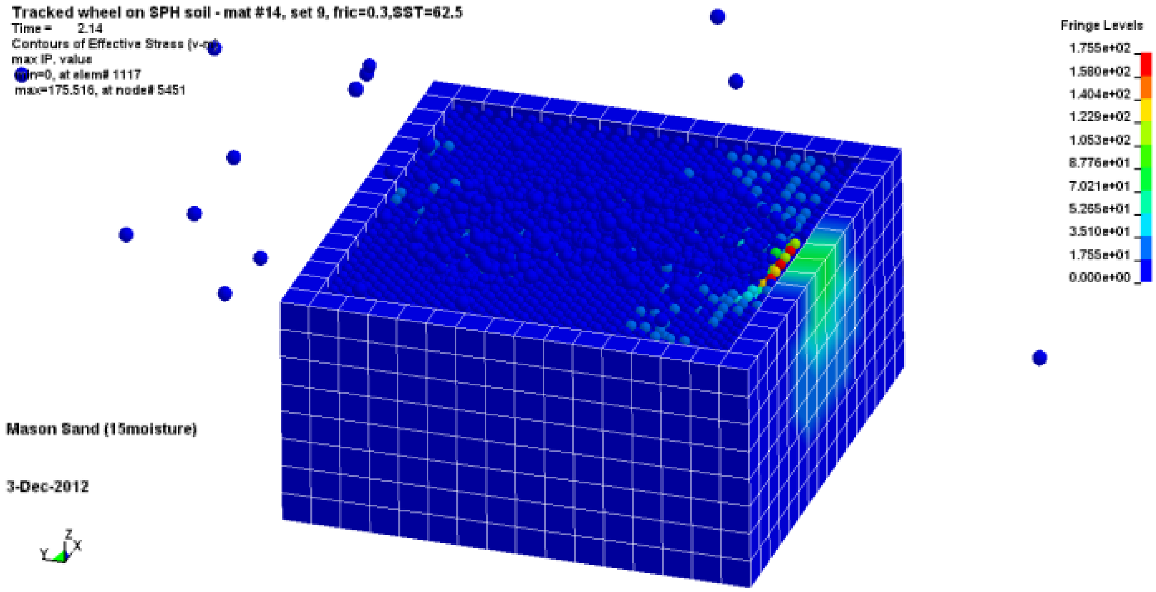


Figure 12b –von Mises stress in substrate (Mason sand, 15% moisture) after analysis

The X-moment and Y-velocity of the wheel are similar to the results from an FEA analysis:

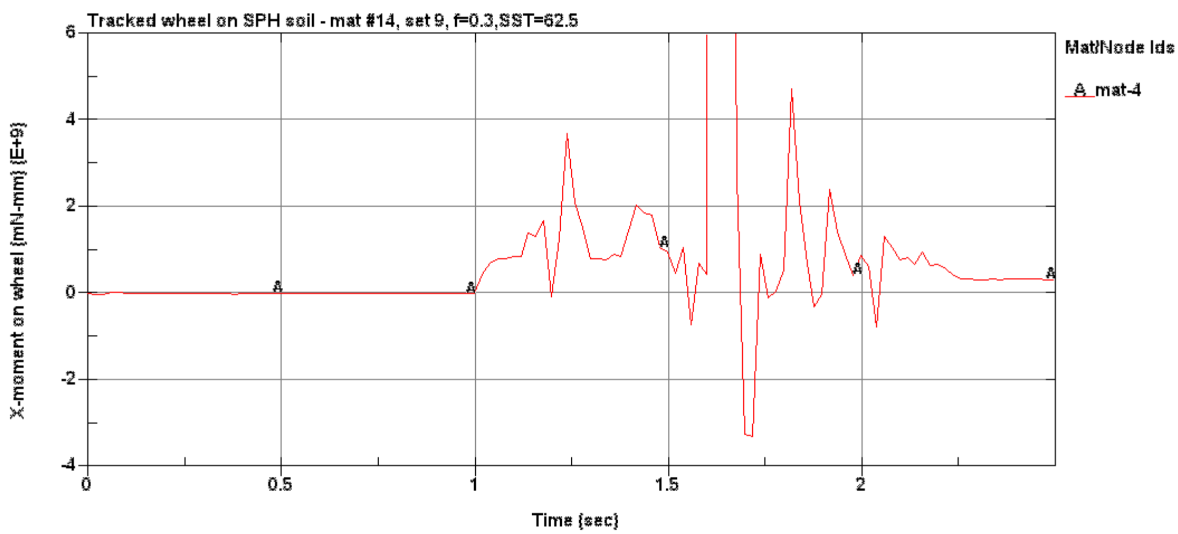


Figure 13a – X-moment of wheel during SPH analysis of Mason sand (15% moisture)

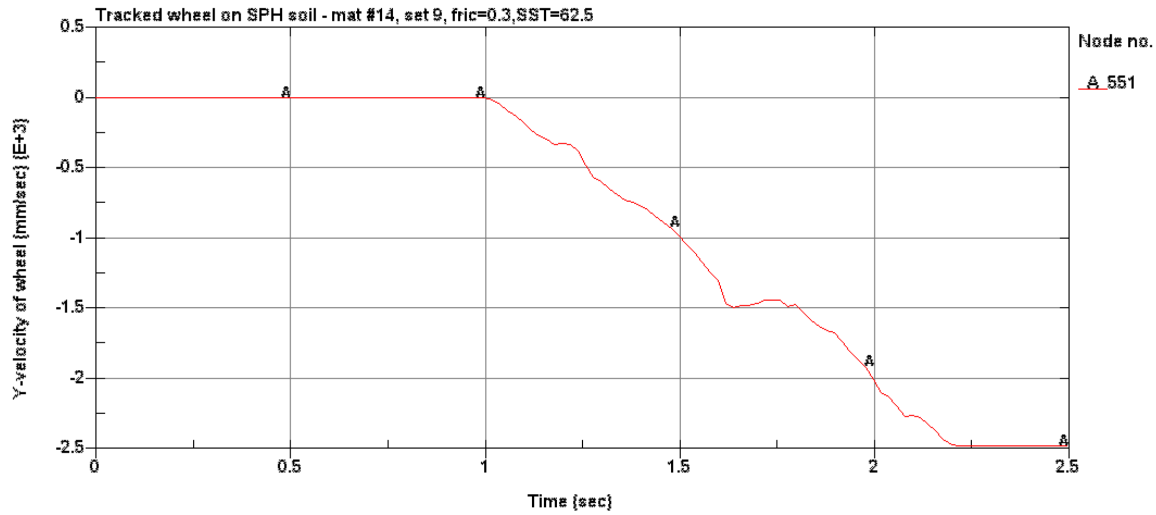


Figure 13b –Y velocity of wheel during SPH analysis of Mason sand (15% moisture)

There is a notable spike in X-moment at about 1.6 sec and corresponding bump in velocity in the above results but the cause is unknown. In general, the X-moment results from SPH analyses are even noisier than those from the FEA runs.

An identical analysis was run using the soil model for Cuddeback A, a dry lakebed soil (Material Type 14, data set 14). This harder material showed lower levels of deformation and correspondingly lower amounts of plastic strain after the wheel had passed. X-moment results were noisier while Y-velocity results were comparable to those obtained for the Mason 15% sand:

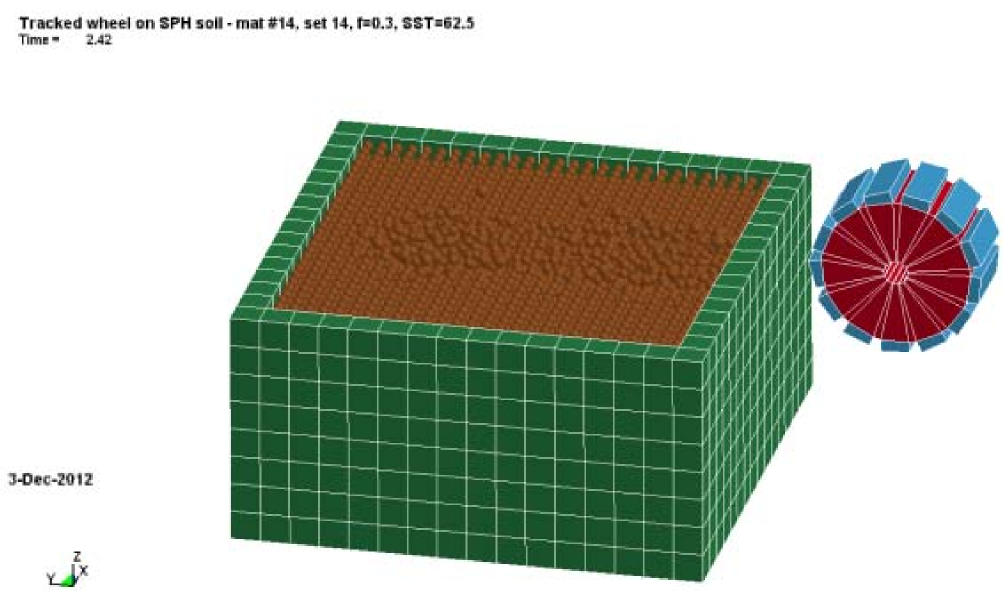


Figure 14a – Deformation after SPH analysis of Cuddeback A soil

 

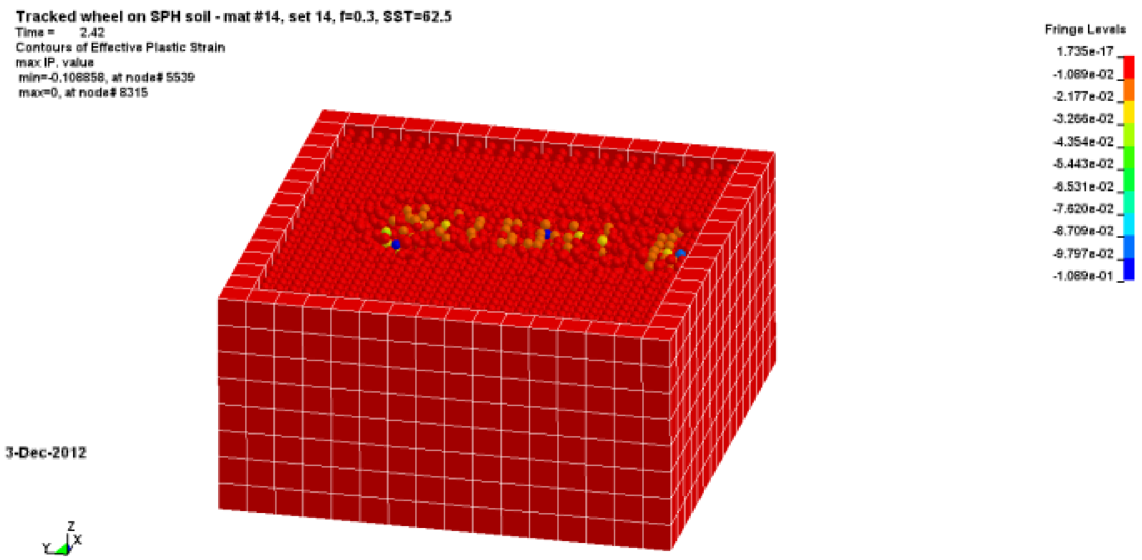


Figure 14b –Plastic strain after SPH analysis of Cuddeback A soil

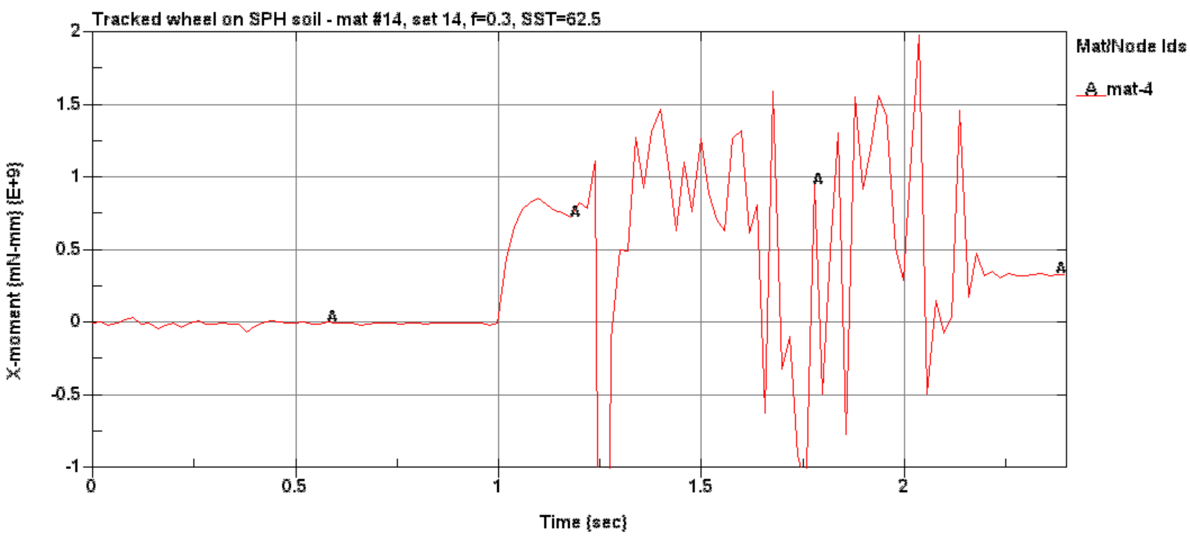


Figure 14c – X-moment of wheel during SPH analysis of Cuddeback A soil

 

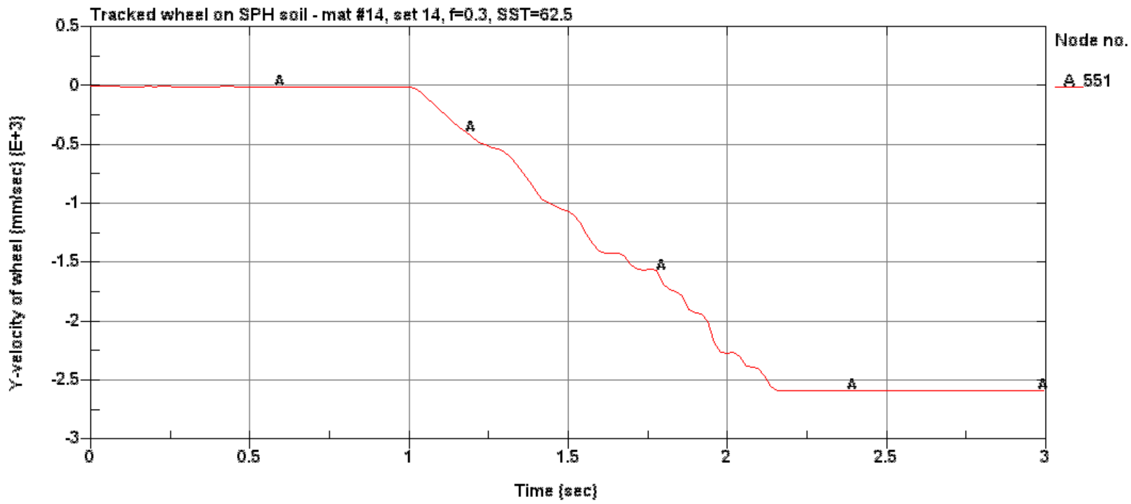


Figure 14d –Y-velocity of wheel during SPH analysis of Cuddeback A soil

Softer substrates were also simulated, with mixed results. The contact instability issue discussed in the previous sections also affected our SPH calculations. Unfortunately, the parameter values that worked so well to address this issue in solid-solid contact did not help as much in SPH calculations and, in fact, seemed to make the problem worse. Figure 15a shows the wheel on KSC dry sand (material type 5, data set 8). It has moved substantially across the substrate after sinking in noticeably during the stabilization period but the result looks good at this point:

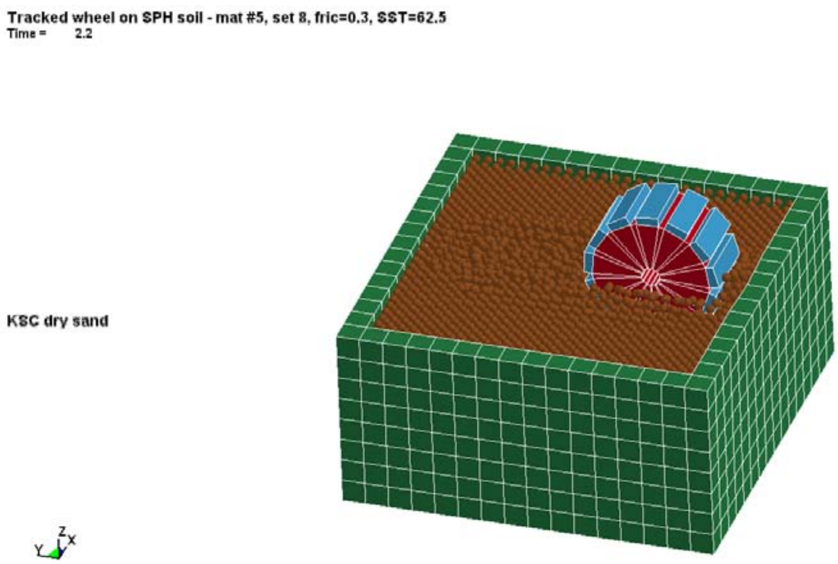


Figure 15a – Tracked wheel travelling on KSC dry sand (Material Type 5, data set 8)

Unfortunately, an instant later a contact instability occurred, terminating the analysis:

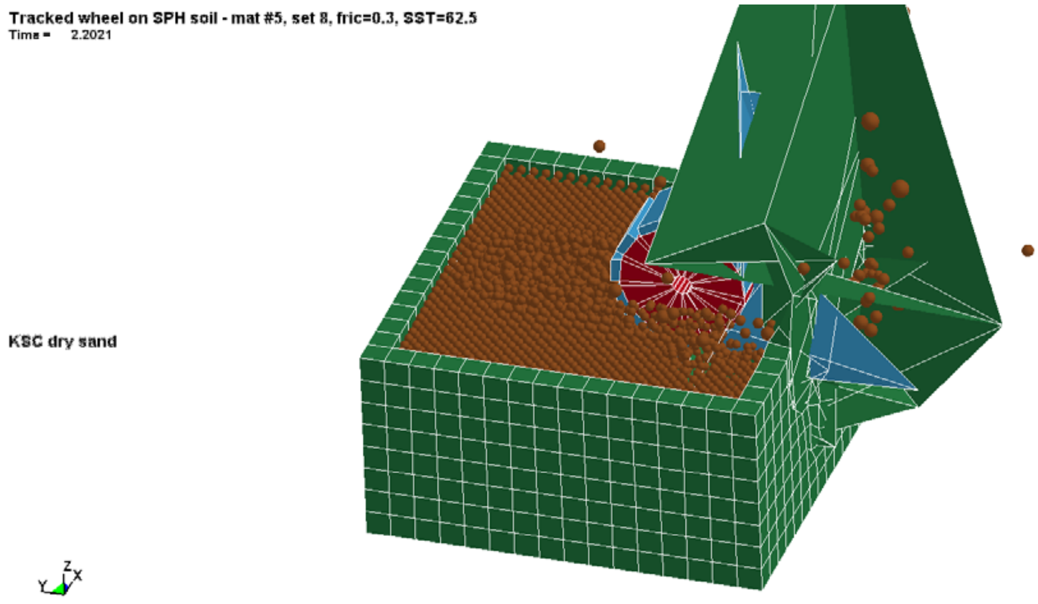


Figure 15b – Contact instability in SPH analysis of KSC dry sand (Material Type 5, data set 8)

A similar model, using Material Type 14, data set 8, also terminated due to a contact instability, but much earlier in the analysis (0.85 sec, cf. 2.2 sec) demonstrating just how unpredictable the instabilities can be:

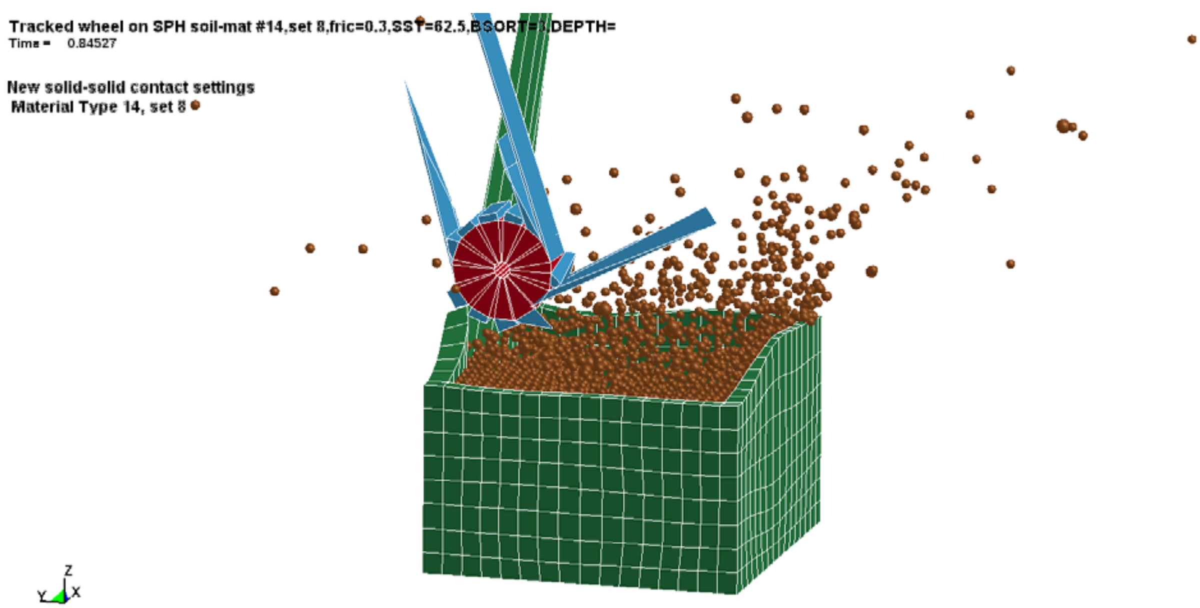


Figure 15c– Contact instability in SPH analysis of KSC dry sand (Material Type 14, data set 8)

Frustratingly, the models appear to be working well right up until the moment of the instability. Hopefully, once this issue is resolved, the good features of the models will be more apparent.

An attempt was made to run a model using a substantially finer SPH mesh (~100K nodes) using the material properties of a firm, moist sand (Kennedy Space Center, material type 5, data set 10). This model ran for about two weeks but at the time of this report had only gone just past the halfway point on the stabilization time period. Nevertheless, the below image of the pad sinking into the SPH material gives an idea as to the relative mesh density between pad shape and SPH spacing:

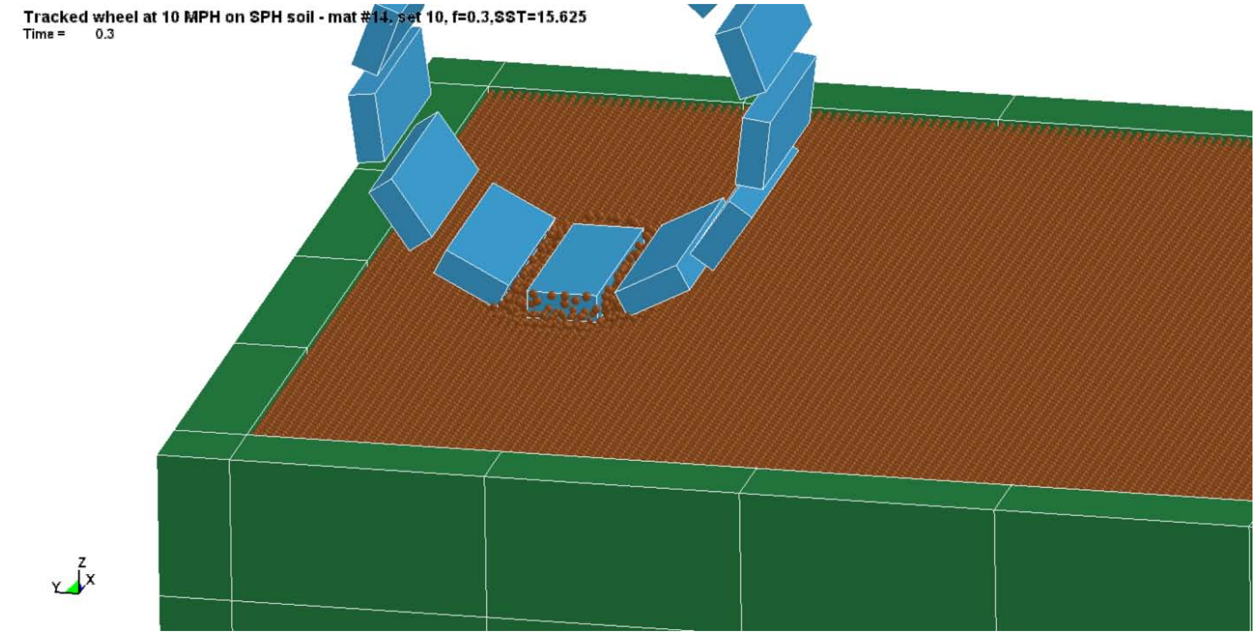


Figure 16 – Track pad on SPH material (KSC moist sand) during stabilization period

The penetration of the SPH nodes between the pads is something that the relatively coarse FEA meshes cannot duplicate as is also the case with the standard SPH mesh density used. For truly soft material simulations increased mesh density will be an essential tool for accuracy.

As extensions to the simple models we used to validate the SPH approach, we tried running two cases that would hopefully show the models' ability to quantify performance under different situations. One of these models had a rotated domain such that the wheel was attempting to climb a 10° slope. The below Figure shows the wheel at a point in the analysis just before terminating due to a contact instability:

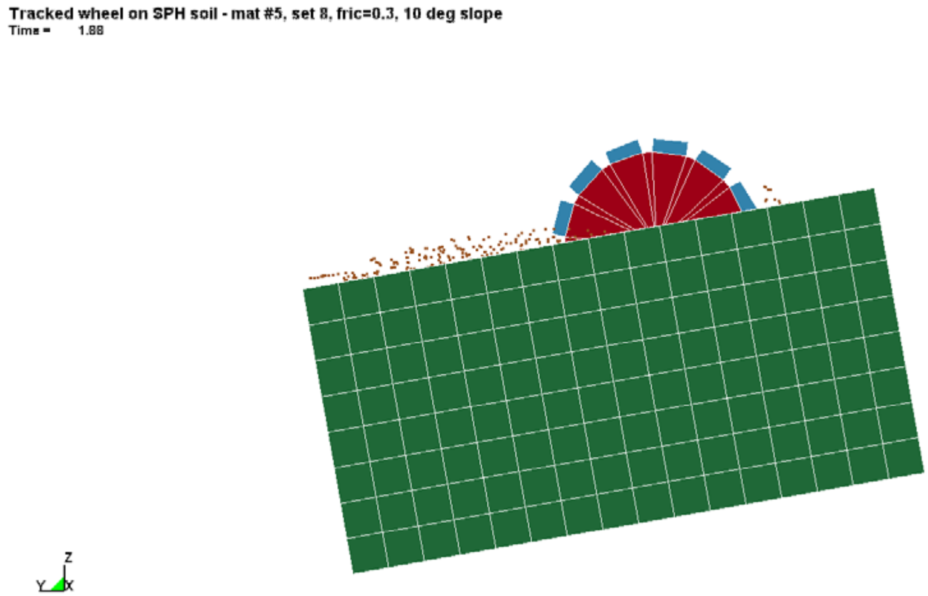


Figure 17a – Tracked wheel in KSC dry sand (Material Type 5, data set 8) at 10° slope

The wheel has dug substantially further into the substrate at this time in the analysis than at 0° slope:

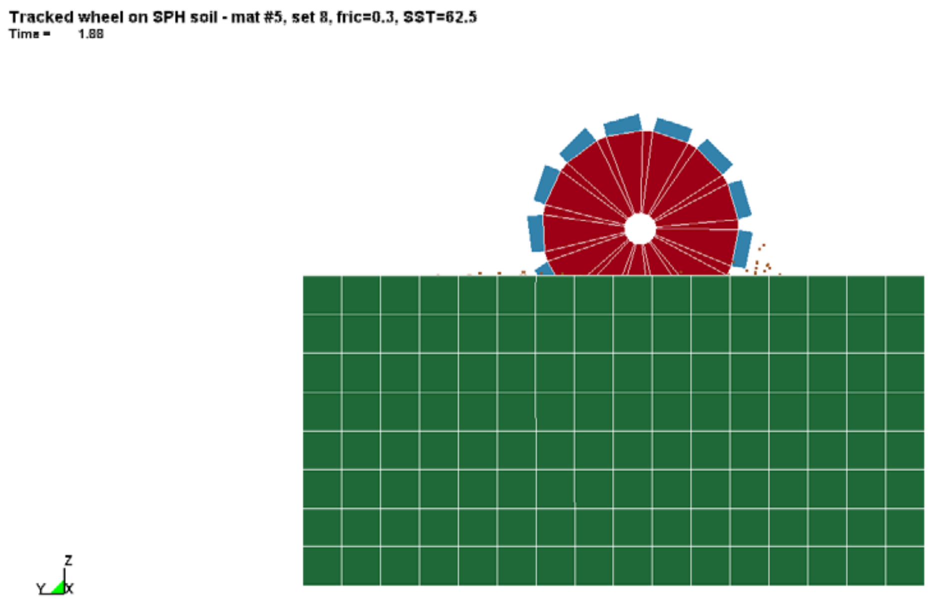


Figure 17b – Tracked wheel in KSC dry sand (Material Type 5, data set 8) at 0° slope at same time

Another model was constructed to handle an extremely rapid acceleration of the wheel to 25MPH over a 1.6 second time period. Under perfect conditions this would take a domain of ~9 m in length to still have the wheel on our substrate. Since our friction coefficient would require a longer length to obtain top velocity, the domain was extended to 15 m in order to allow the wheel to reach as close to its top velocity as possible (Figure 18).

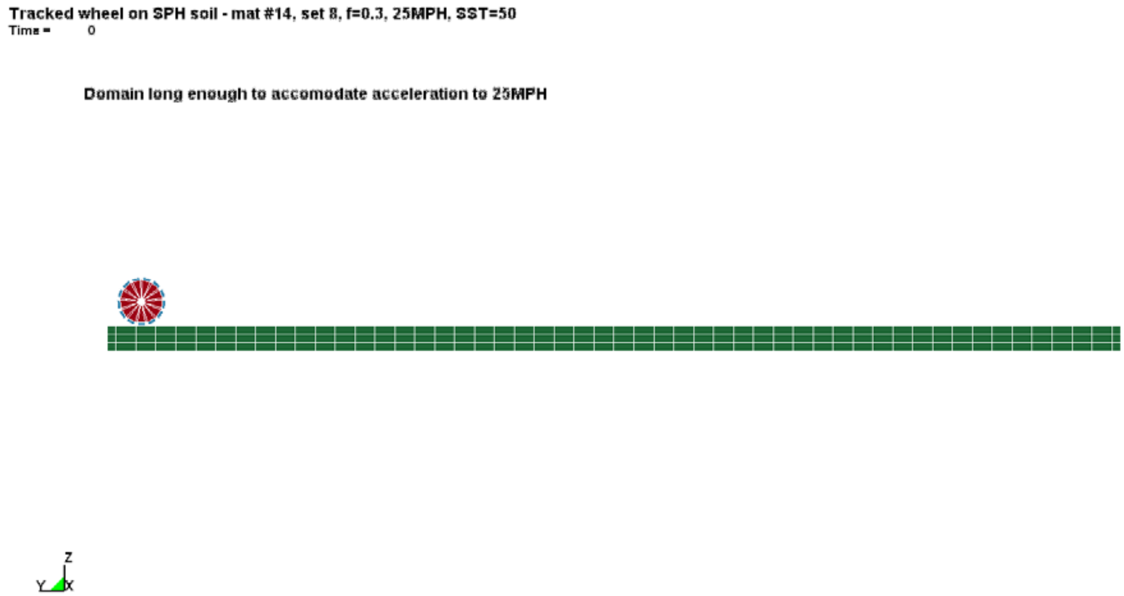


Figure 18 – Domain used for analysis of wheel accelerating to 25 MPH (11.2 m/s) in 1.6 sec

At the time of this report, the model had only reached ~0.9 seconds (0.4 seconds into the acceleration) but the results show a substantial ejection of SPH material behind the wheel due to the rapid acceleration and the wheel is digging its way into the substrate:

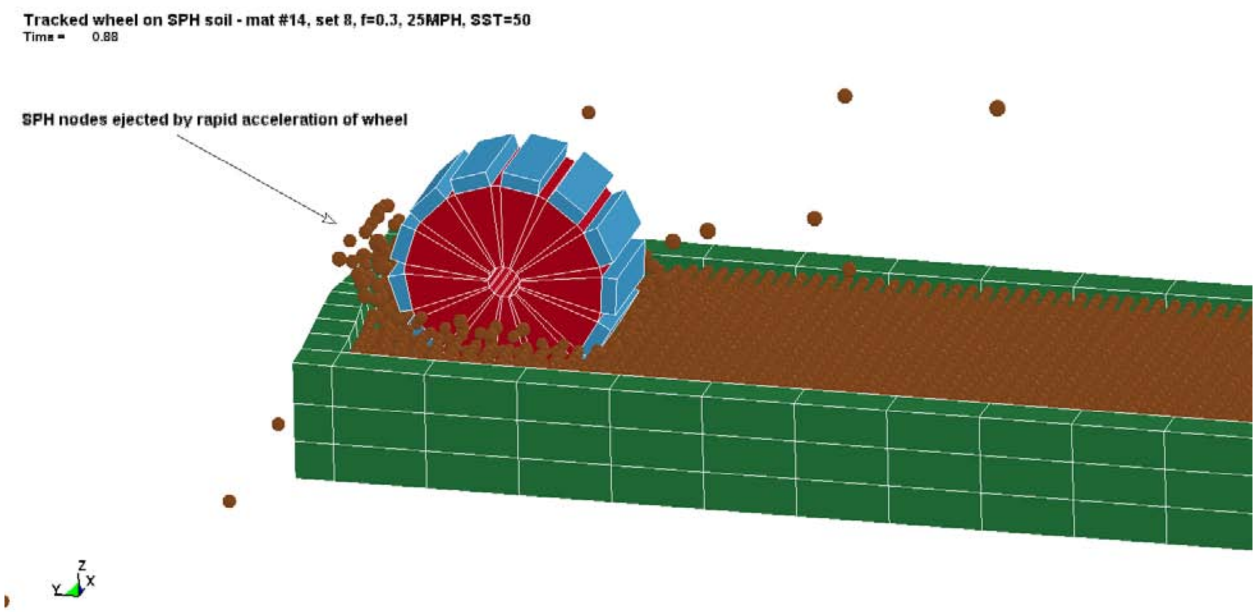


Figure 18a – SPH nodes being ejected behind rapidly accelerating wheel

These two model extensions demonstrate that even these simple SPH models can produce results showing the qualitative differences between parameters such as slope and acceleration rates. In the sloped case, the wheel dug itself deeper into the substrate, a result seen on actual tracked vehicles. In the high acceleration case, more substantial amounts of material were ejected by the track pads than at the more modest acceleration rates used in other models.

## 1.4 Important Findings and Conclusions

For the general problem of simulating tracked wheels on substrates, the following solution strategies should be used:

> For substrate materials that are quite hard (e.g. dry lakebed soils) typical solid elements should suffice for many analyses using solid-solid contact to address the interactions between track pads and the substrates. For hard materials that are more complex than the SOIL_AND_FOAM model in LS-DYNA is capable of representing, there are many alternative models in LS-DYNA that can be used.
>
> For very soft materials (e.g. muds and soft sands) SPH technology should be employed as it would be the preferred mesh-free method to handle the extreme deformations likely to occur in these materials. Materials that are so soft that they easily are stressed into a "failed" regime where only their mass remains important is a situation very appropriate for SPH technology.
>
> For those materials of intermediate hardness there are several alternatives. An eroding solid element contact approach could be used as well as the SPH method with the SPH method probably being more straightforward to implement.

The SPH models we have been able to successfully execute demonstrate an ability to capture the qualitative features we would expect for a tracked wheel on soft substrates. Ejection of the material from the domain, substantial sinking into the substrate and the formation of a "bulge" of material in front of the wheel have all been seen in these SPH analyses. After correcting our issue with contact instability the next step will be to refine the SPH models so as to obtain real, quantitative results for actual tracked wheel designs.

The most significant issue in this project involves the contact instabilities that produce the anomalous forces causing model termination. The good news is that we may have a solution in hand for solid-solid contact with the new parameter values. However, this will require extensive verification to be sure the solution is sufficiently robust and we still need to address its persistence in SPH models.

The contact instability issue is presumably present and lurking in all SPH models, but is also potentially correctable. However, we have simply run out of time to validate any further potential solutions from LSTC. There is one possible solution that should be attempted at the next opportunity (there was no time left in the project to validate it). The idea is to simply remove the solid-solid contact definitions from the input file and to expand the SPH domain so that the wheel will not encounter any of the other solid elements during the analysis. This idea was suggested by the observation that just about every instance of the contact instabilities that occurs appears to involve solid-solid contact. This may be incorrect but it is worth pursuing in a couple of models to see if the instability can be avoided. This will carry a price in computational efficiency. Before going too far down this path, however, it is critical to continue working with LSTC support to confirm that the issue in these models is actually the solid-solid contact and not something else (e.g. SPH-solid contact).

When the instability does not present itself, we appear to have a functional set of analysis parameters that enables us to perform reasonable SPH analyses of tracked wheels on hard soils. Qualitatively the results look reasonable but further work needs to be done to refine the SPH mesh and determine how to obtain smoother X-moment results, which are almost useless in their current form. It may be possible to obtain results on soft substrates but those analyses have a high risk of being interrupted by contact instabilities.

Lastly, the SPH models in total offer a caution as to what level of CPU resources would be required to accurately simulate actual tracked vehicles on soft substrates for long periods of time (seconds). The combination of high acceleration rates/velocities, different track pad designs and soft soils will require the models to have long domain lengths, high SPH mesh density and deep SPH domains to accommodate settling/digging of the tracked wheels. The requirement for uniform SPH mesh density will mean that million node meshes will be required, at a minimum, to perform these analyses. It is worth noting that the SPH capability is compatible with the MPP (Massively Parallel Processing) version of LS-DYNA so it may be possible to reduce the computation times substantially on the right kind of equipment. As a first step to reduce the computational burden, symmetries in the SPH models need to be utilized to the maximum possible extent. Use should also be made of LS-DYNA commands that ignore SPH nodes a certain distance beyond the model.

## 1.5 Implications for Further Research

The DEM (Discrete Element Method) should also be evaluated as an analysis technique. For complex materials that are firm enough to not be instantly obliterated by the track pads it may provide more quantitative results than an SPH approach. LS-DYNA has a DEM capability under development but there are other commercial codes that could be used instead.

While a number of soil and sand data sets were accumulated during this project we did not find a comprehensive model that could describe a material over, say, an entire moisture range from dry to thoroughly wet. One of the materials notably absent from our collection of data is wet mud, a substance that tracked vehicles are likely to encounter.

The friction coefficients used in these analyses were averaged values from one reference. Presumably, there exists a more comprehensive set of friction data for track pads on a wide variety of soils or one can obtain such data experimentally. The role of that parameter was not investigated at all here but would be an obvious target for inclusion into a proper Design Of Experiments evaluation of the general problem.

Adaptive Solid to SPH elements is a technology that should also be pursued further, but in close cooperation with LSTC support personnel and after our other issues with SPH contact have been resolved. While the primary issues we encountered appear to be contact driven, there is still a lack of clarity from LSTC documentation on just what “coupling” between the newly-liberated SPH nodes and solid elements actually entails which makes it difficult to determine just what combination of ICPL and IOPT parameters most closely describes our physical situation. Again, this should be a tractable issue that can be resolved with further communication with LSTC.

## 1.6 References

Chitty, M. A. (2011). *Constitutive Soil Properties for Mason Sand and Kennedy Space Center NASA/CR-2011-217323.* Albuquerque, NM: Applied Research Associates, Inc.

Guo, Y. (2010). Meshless Methods in LS-DYNA: an Overview of EFG and SPH. Stuttgart, Germany: LSTC.

Hallquist, J. (2006). *LS-DYNA Theory Manual.* Livermore, CA: LSTC.

Kulak, R. F., & Schwer, L. (2012). Effect of Soil material Models on SPH Simulations for Soil-Structure Interaction. *12th International LS-DYNA Users Conference.* Detroit, MI.

Lescoe, R. (2010). *Improvement of soil modeling in a tire-soil interaction using Finite Element Analysis and Smooth Particle Hydrodynamics - MS Thesis.* Penn State University.

Livermore Software Technology Corporation. (2012). *LS-DYNA Keyword User's Manual Volume 1 Version 971.* Livermore, CA.

Schwer, L. (2012, November 16). Personal communication.

Tekeste, M. Z., Raper, R. L., Tollner, E. W., & Way, T. R. (2005). Effect of Soil Moisture, Soil Density, and Cone Penetrometer Material on Finite Element Prediction of Soil Hardpan Depth (Paper #: 051164). *ASAE Annual International Meeting* (p. 9 (Table 4)). Tampa, FL: American Society of Agricultural Engineers.

## 1.7 Annex - Material Models used in Simulations

Several material types and data sets have been used in the SPH modeling of soils. In LS-DYNA terminology, these can be described as:

Material Type 5, Soil and Foam

Material Type 9, Null Material

Material Type 10, Elastic Plastic Hydro(dynamic)

Material Type 14, Soil and Foam Failure

Material Type 25, Inviscid Two Invariant Geologic Cap

Material Type 79 (Hysteretic Soil (Elasto-Perfectly Plastic))

These are part of the wide variety of material models appropriate for soil available in LS-DYNA but appear to cover the range of constitutive relations used in published SPH simulations involving soil. The vast majority of our analyses were performed on materials of Type 5 or 14. Material Type 14 is a version of Material Type 5 where the material loses its ability to carry tension when the PC (pressure cutoff) value is exceeded. The input data for Material Type 14 is the same as for Material Type 5.

An equation of state is required in SPH analyses to address the pressure-volume relationship in compression. For the Type 5 or 14 materials this is addressed by the P vs. ln (vol. strain) data. For other constitutive models a specific EOS must be chosen from the number of models available in LS-DYNA. Most of the EOS models in LS-DYNA are designed to be compatible with shock waves. Due to the relatively low-speed nature of track/substrate interactions (very low Mach number) the simplest form of EOS is all that is required. For those constitutive models that required an EOS we used the simplest representation (Linear Polynomial) with only non-zero coefficient C2=K (bulk modulus).

Below is a set of tables listing explicit values for the various material model data sets found in a brief review of the literature, organized by Material Type. Parameter values are listed with the units used in the simulations (mm-mN-kg-sec system).

**Material Type 5 (Soil and Foam)**

Kulak, R. F.; Bojanowski, C. 'Modeling of cone Penetration Test Using SPH and MM-ALE Approaches' 8th European LS-DYNA® Users Conference, Strasbourg (May, 2011) (Table 1)

| Description | Norfolk Sandy Loam | Set 1 |
|---|---|---|
| Variable | Value | Units |
| Density (RO) | 1.255e-6 | kg/mm$^3$ |
| G | 1724 | mN/mm$^2$ |
| K | 5516 | mN/mm$^2$ |
| A0 | 0 | |
| A1 | 0 | |
| A2 | 0.8702 | |
| PC | 0 | |
| VCR | 0 (on) | |
| REF | 0 (off; ref. geometry) | |
| -ln(V/V0) | 0, 0.12783, 0.19845, 0.24846, 0.31471, 0.40048 | |
| P | 0, 50, 100, 150, 250, 500 | mN/mm$^2$ |

Kulak, R. F.; Schwer, L. 'Effect of Soil Material Models on SPH Simulations for Soil-Structure Interaction' 12th International LS-DYNA® Users Conference (Table 2, Figures 1&2)

| Description | Soil | Set 2 |
|---|---|---|
| Variable | Value | Units |
| Density (RO) | 1.64e-6 | kg/mm$^3$ |
| G | 136000 | mN/mm$^2$ |
| K | 4700000 | mN/mm$^2$ |
| A0 | 0 | |
| A1 | 0 | |
| A2 | 0.3736 | |
| PC | 0 | |
| VCR | 0 (on) | |
| REF | 0 (off; ref. geometry) | |
| -ln(V/V0) | 0,0.02,0.04,0.06,0.08,0.1,0.15,0.20,0.25,0.30 | |
| P | 0,7912.1,14945,22857,29011,35165,53846,84615,142308,242308 | mN/mm$^2$ |

Barsotti, M. A.; Puryear, J. M. H.; Stevens, D. J.; Alberson, R. M.; McMahon, P. "Modeling Mine Blast with SPH" 12th International LS-DYNA® Users Conference

| Description | Soil | Set 3 |
|---|---|---|
| Variable | Value | Units |
| Density (RO) | 1.37e-6 | kg/mm³ |
| G | 3.6 | mN/mm² |
| K[1] | | mN/mm² |
| A0 | 25300 | (mN/mm²)² |
| A1 | | mN/mm² |
| A2 | | |
| PC | -34.47 | mN/mm² |
| VCR | 1 (off) | |
| REF | 0 | |

With Pressure vs. Volumetric Strain data shown below:

| Strain | ln(1-strain) | P (mN/mm²) |
|---|---|---|
| 0.00000 | 0 | 0.00 |
| 0.00563 | -0.0056409 | 198.11 |
| 0.01031 | -0.010366 | 278.30 |
| 0.01500 | -0.0151136 | 325.47 |
| 0.01969 | -0.0198839 | 358.49 |
| 0.02531 | -0.0256384 | 377.36 |
| 0.03000 | -0.0304592 | 396.23 |
| 0.06094 | -0.0628732 | 438.68 |
| 0.10500 | -0.1109316 | 452.83 |
| 0.11625 | -0.1235811 | 457.55 |

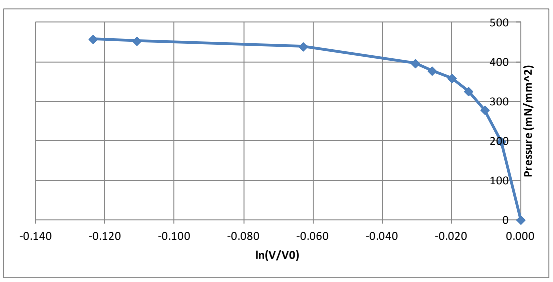


[1] DYNA automatically calculates a value of K (35120) from the first two data points of the P vs. ln(1-strain) table.

Bojanowski, C.; Kulak, R. F. 'Comparison of Lagrangian, SPH and MM-ALE Approaches for Modeling Large Deformations in Soil' 11th International LS-DYNA® Users Conference (2010) (Table 1, Figure 3):

| Description | Loose, silty clay sand | Set 4 |
|---|---|---|
| Variable | Value | Units |
| Density (RO) | 2.359e-6 | kg/mm$^3$ |
| G | 34474 | mN/mm$^2$ |
| K | 15024 | mN/mm$^2$ |
| A0 | 0 | |
| A1 | 0 | |
| A2 | 0.602 | |
| PC | 0 | |
| VCR | 0 (on) | |
| REF | 0 (off; ref. geometry) | |
| -ln(V/V0) | 0,0.023,0.04,0.06,0.07,0.08,0.088,0.101,0.112,0.128 | |
| P | 0,80,130,280,350,405,490,610,700,900 | mN/mm$^2$ |

Fasanella, E. L.; Lyle, K. H.; Jackson, K. E. "Developing Soil Models for Dynamic Impact Simulations" (Table 2, Figure 14)

| Description | Unwashed Sand | Set 5 |
|---|---|---|
| Variable | Value | Units |
| Density (RO) | 2.095e-6 | kg/mm$^3$ |
| G | 23029 | mN/mm$^2$ |
| K | 133556 | mN/mm$^2$ |
| A0 | 300.7 | (mN/mm$^2$)$^2$ |
| A1 | 25.56 | mN/mm$^2$ |
| A2 | 0.543 | |
| PC | -6.895 | mN/mm$^2$ |
| VCR | 0 (on) | |
| REF | 0 (off; ref. geometry) | |
| -ln(V/V0) | 0,0.00251,0.00474,0.007,0.0092,0.0103,0.0114,0.0125,0.0137,0.016 | |
| P | 0,66.73,137.16,203.88,274.32,311.39,344.75,378.11,411.48,489.32 | mN/mm$^2$ |

Fasanella, E. L.; Lyle, K. H.; Kellas, S. “Soft Soil Impact Testing and Simulation of Aerospace Structures” 10th International LS-DYNA® Users Conference (Table 1, Figure 5)

| Description | Soft Soil | Set 6 |
|---|---|---|
| Variable | Value | Units |
| Density (RO) | 1.4535e-6 | $kg/mm^3$ |
| G | 1841 | $mN/mm^2$ |
| K | 68950 | $mN/mm^2$ |
| A0 | 0 | $(mN/mm^2)^2$ |
| A1 | 0 | $mN/mm^2$ |
| A2 | 0.3 | |
| PC | 0 | $mN/mm^2$ |
| VCR | 0 (on) | |
| REF | 0 (off; ref. geometry) | |
| -ln(V/V0) | 0,0.00396,0.0119,0.032,0.0568,0.0891,0.12,0.157 | |
| P | 0,7.51,13.94,27.89,41.83,55.24,68.64,82.59 | $mN/mm^2$ |

Palmer, T.; Honken, B.; Chou, C.; ‘Rollover Simulations for Vehicles using Deformable road Surfaces’ 12th International LS-DYNA® Users Conference (Page 8)

| Description | Damp Sand | Set 7 |
|---|---|---|
| Variable | Value | Units |
| Density (RO) | 1.6e-6 (assumed; not listed) | $kg/mm^3$ |
| G | 11800 | $mN/mm^2$ |
| K | 107500 | $mN/mm^2$ |
| A0 | 0 | |
| A1 | 0 | |
| A2 | 0.6 | |
| PC | 0 | |
| VCR | 0 (on) | |
| REF | 0 (off; ref. geometry) | |
| -ln(V/V0) | 0,0.006,0.009,0.012,0.015,0.018,0.021,0.024,0.027,0.030 | |
| P | 0,79.2,194.4,329.2,548.5,740.5,1024.5,1284.7,1562.2,1925.2 | $mN/mm^2$ |

  

Chitty, M. A. (2011). Constitutive Soil Properties for Mason Sand and Kennedy Space Center NASA/CR-2011-217323. Albuquerque, NM: Applied Research Associates, Inc. (Page 41)

| Description | KSC Low Density, Dry Sand | Set 8 |
|---|---|---|
| Variable | Value | Units |
| Density (RO) | 1.2835e-6 | $kg/mm^3$ |
| G | 508.1615 | $mN/mm^2$ |
| K | 257804.05 | $mN/mm^2$ |
| A0 | 4.2687086 | $(mN/mm^2)^2$ |
| A1 | 2.915206 | $mN/mm^2$ |
| A2 | 0.4978 | |
| PC | -3.4475 | $mN/mm^2$ |
| VCR | 0 (on) | |
| REF | 0 (off; ref. geometry) | |
| -ln(V/V0) | 0,0.01586,0.3794,0.04539,0.0525,0.05748,0.0656,0.0694,0.0732 | |
| P | 0,18.51,19.65,125.08,128.66,228.91,337.17,607.1,767,929.45 | $mN/mm^2$ |

Chitty, M. A. (2011). Constitutive Soil Properties for Mason Sand and Kennedy Space Center NASA/CR-2011-217323. Albuquerque, NM: Applied Research Associates, Inc. (Page 110)

| Description | KSC Mason Sand, 15% moisture | Set 9 |
|---|---|---|
| Variable | Value | Units |
| Density (RO) | 1.8397e-6 | $kg/mm^3$ |
| G | 13755.525 | $mN/mm^2$ |
| K | 431489.1 | $mN/mm^2$ |
| A0 | 62.896776 | $(mN/mm^2)^2$ |
| A1 | 13.962375 | $mN/mm^2$ |
| A2 | 0.7752 | |
| PC | -6.895 | $mN/mm^2$ |
| VCR | 0 (on) | |
| REF | 0 (off; ref. geometry) | |
| -ln(V/V0) | 0,0.001,0.002,0.003,0.004,0.005,0.006,0.007,0.008,0.0092 | |
| P | 0,21.175,66.985,136.935,231.258,355.437,506.507,687.983,895.66, 1181.11 | $mN/mm^2$ |

 

Chitty, M. A. (2011). Constitutive Soil Properties for Mason Sand and Kennedy Space Center NASA/CR-2011-217323. Albuquerque, NM: Applied Research Associates, Inc. (Page 58)

| Description | KSC High Density In-situ moisture Sand | Set 10 |
|---|---|---|
| Variable | Value | Units |
| Density (RO) | 1.6044e-6 | $kg/mm^3$ |
| G | 9701.265 | $mN/mm^2$ |
| K | 299436.06 | $mN/mm^2$ |
| A0 | 67.555797 | $(mN/mm^2)^2$ |
| A1 | 11.95593 | $mN/mm^2$ |
| A2 | 0.5290 | |
| PC | -6.895 | $mN/mm^2$ |
| VCR | 0 (on) | |
| REF | 0 (off; ref. geometry) | |
| -ln(V/V0) | 0,0.001,0.002,0.003,0.004,0.006,0.008,0.01,0.012,0.01394 | |
| P | 0,17.493,49.582,89.635,138.727,259.804,414.665,586.558,780.514, 978.4 | $mN/mm^2$ |

Chitty, M. A. (2011). Constitutive Soil Properties for Mason Sand and Kennedy Space Center NASA/CR-2011-217323. Albuquerque, NM: Applied Research Associates, Inc. (Page 74)

| Description | Mason 4% water | Set 11 |
|---|---|---|
| Variable | Value | Units |
| Density (RO) | 1.615e-6 | $kg/mm^3$ |
| G | 12080.04 | $mN/mm^2$ |
| K | 389360.65 | $mN/mm^2$ |
| A0 | 64.750876 | $(mN/mm^2)^2$ |
| A1 | 13.176345 | $mN/mm^2$ |
| A2 | 0.6700 | |
| PC | -3.4475 | $mN/mm^2$ |
| VCR | 0 (on) | |
| REF | 0 (off; ref. geometry) | |
| -ln(V/V0) | 0,0.001,0.002,0.003,0.004,0.005,0.006,0.007,0.009,0.01031 | |
| P | 0,19.03,58.125,98.323,196.439,296.209,413.011,545.739,866.219, 1108.716 | $mN/mm^2$ |

Chitty, M. A. (2011). Constitutive Soil Properties for Mason Sand and Kennedy Space Center NASA/CR-2011-217323. Albuquerque, NM: Applied Research Associates, Inc. (Page 86)

| Description | Mason 8% water | Set 12 |
|---|---|---|
| Variable | Value | Units |
| Density (RO) | 1.6578e-6 | $kg/mm^3$ |
| G | 16368.73 | $mN/mm^2$ |
| K | 347825.17 | $mN/mm^2$ |
| A0 | 65.036122 | $(mN/mm^2)^2$ |
| A1 | 13.203925 | $mN/mm^2$ |
| A2 | 0.6700 | |
| PC | -3.4475 | $mN/mm^2$ |
| VCR | 0 | |
| REF | 0 (off; ref. geometry) | |
| -ln(V/V0) | 0,0.001,0.002,0.003,0.004,0.005,0.006,0.007,0.009,0.01044 | |
| P | 0,26.270,65.296,121.904,196.025,291.521,401.565,530.846, 851.050,1116.507 | $mN/mm^2$ |

Chitty, M. A. (2011). Constitutive Soil Properties for Mason Sand and Kennedy Space Center NASA/CR-2011-217323. Albuquerque, NM: Applied Research Associates, Inc. (Page 98)

| Description | Mason 5% water | Set 13 |
|---|---|---|
| Variable | Value | Units |
| Density (RO) | 1.6792e-6 | $kg/mm^3$ |
| G | 24539.305 | $mN/mm^2$ |
| K | 493544.1 | $mN/mm^2$ |
| A0 | 62.421366 | $(mN/mm^2)^2$ |
| A1 | 14.279545 | $mN/mm^2$ |
| A2 | 0.8164 | |
| PC | -3.4475 | $mN/mm^2$ |
| VCR | 0 | |
| REF | 0 (off; ref. geometry) | |
| -ln(V/V0) | 0,0.001,0.002,0.003,-0.004,0.005,0.006,0.007,0.008,0.00861 | |
| P | 0,36.930,99.357,187.682,308.275,455.277,635.374,845.327, 1083.205,1236.274 | $mN/mm^2$ |

20080045436_2008045156 NASA report - Constitutive Soil Properties for Cuddeback Lake, CA and Carson Sink, NV (Page 54)

| Description | Cuddeback A | Set 14 |
|---|---|---|
| Variable | Value | Units |
| Density (RO) | 1.4546e-6 | kg/mm$^3$ |
| G | 17237.5 | mN/mm$^2$ |
| K | 119973 | mN/mm$^2$ |
| A0 | 3685.3803 | (mN/mm$^2$)$^2$ |
| A1 | 105.2177 | mN/mm$^2$ |
| A2 | 0.7510 | |
| PC | -13.79 | mN/mm$^2$ |
| VCR | 0 (on) | |
| REF | 0 (off; ref. geometry) | |
| -ln(V/V0) | 0,0.0089,0.0104,0.012,0.0138,0.0155,0.019,0.0226,0.0263,0.0291 | |
| P | 0,206.85,241.325,275.8,310.275,344.75,413.7,482.65, 551.6,605.381 | mN/mm$^2$ |

20080045436_2008045156 NASA report - Constitutive Soil Properties for Cuddeback Lake, CA and Carson Sink, NV (Page 73)

| Description | Cuddeback B | Set 15 |
|---|---|---|
| Variable | Value | Units |
| Density (RO) | 1.2942e-6 | kg/mm$^3$ |
| G | 3171.7 | mN/mm$^2$ |
| K | 168238 | mN/mm$^2$ |
| A0 | 6.1803333 | (mN/mm$^2$)$^2$ |
| A1 | 5.14367 | mN/mm$^2$ |
| A2 | 1.0680 | |
| PC | 0 | mN/mm$^2$ |
| VCR | 0 (on) | |
| REF | 0 (off; ref. geometry) | |
| -ln(V/V0) | 0,0.0222,0.0317,0.0379,0.0436,0.0491,0.0592,0.0683,0.0766,0.0827 | |
| P | 0,124.11,172.375,206.85,241.325,275.8,344.75,413.7, 482.65,537.81 | mN/mm$^2$ |

  

**Material Type 9 (Null Material)**

The Null Material model can be constructed from any soil model that has a density and a bulk modulus available. For example, Data Set 5 from Material Type 5 above would have these values as a NULL material:

| Description | Unwashed Sand | |
|---|---|---|
| Variable | Value | Units |
| Density (RO) | 2.095e-6 | kg/mm$^3$ |
| K | 133556 | mN/mm$^2$ |

**Material Type 10 (Elastic Plastic Hydrodynamic)**

Kulak, R. F.; Schwer, L. 'Effect of Soil Material Models on SPH Simulations for Soil-Structure Interaction' 12$^{th}$ International LS-DYNA® Users Conference (Table 2, Figures 1&2)

| Description | Soil | |
|---|---|---|
| Variable | Value | Units |
| Density (RO) | 1.64e-6 | kg/mm$^3$ |
| G | 136000 | mN/mm$^2$ |
| PC | -510 | mN/mm$^2$ |
| A1 | 1057.8 | mN/mm$^2$ |
| -ln(V/V0) | 0,0.02,0.04,0.06,0.08,0.1,0.15,0.20,0.25,0.30 | |
| P | 0,7912.1,14945,22857,29011,35165,53846,84615,142308,242308 | mN/mm$^2$ |

Lescoe, R. "Improvement of soil modeling in a tire-soil interaction using finite element analysis and smooth particle hydrodynamics" Master's Thesis, Penn State University, 2010.

| Description | Dense Sand/Sandy Loam | |
|---|---|---|
| Variable | Value | Units |
| Density | 1.60e-6 | kg/mm$^3$ |
| E | 22000 | mN/mm$^2$ |
| K | 15000 | mN/mm$^2$ |
| G | 9000 | mN/mm$^2$ |
| Yield Stress Y | 16 | mN/mm$^2$ |
| Hardening Modulus | 100 | mN/mm$^2$ |

For an Equation of State, Lescoe used a linear polynomial with the only non-zero coefficient C1=K.

**Material Type 25 (Inviscid Two Invariant Geologic Cap)**

Kulak, R. F.; Schwer, L. 'Effect of Soil Material Models on SPH Simulations for Soil-Structure Interaction' 12th International LS-DYNA® Users Conference (Table 2)

| Description | Soil | |
|---|---|---|
| Variable | Value | Units |
| Density (RO) | 1.64e-6 | $kg/mm^3$ |
| G | 5289000 | $mN/mm^2$ |
| K | 15000000 | $mN/mm^2$ |
| Theta | 0.20375 | radians |
| R | 2.3 | |
| D | 1.6e-3 | |
| W | 0.49 | |
| X0 | 46500 | $mN/mm^2$ |